AD_____

Award Number: DAMD17-98-1-8569

TITLE: Transgenic Models for Prostate Cancer

PRINCIPAL INVESTIGATOR: Charles L. Sawyers, M.D.

CONTRACTING ORGANIZATION: UCLA-Medicine, Hematology/Oncology
Los Angeles, California 90095-1678

REPORT DATE: February 2002

TYPE OF REPORT: Annual Summary

PREPARED FOR: U.S. Army Medical Research and Materiel Command
Fort Detrick, Maryland 21702-5012

DISTRIBUTION STATEMENT: Approved for Public Release;
Distribution Unlimited

The views, opinions and/or findings contained in this report are those of the author(s) and should not be construed as an official Department of the Army position, policy or decision unless so designated by other documentation.

REPORT DOCUMENTATION PAGE

Form Approved
OMB No. 074-0188

1. AGENCY USE ONLY (Leave blank)	2. REPORT DATE	3. REPORT TYPE AND DATES COVERED
	February 2002	Annual Summary (1 Feb 01 - 31 Jan 02)

4. TITLE AND SUBTITLE
Transgenic Models for Prostate Cancer

5. FUNDING NUMBERS
DAMD17-98-1-8569

6. AUTHOR(S) :
Charles L. Sawyers, M.D.

7. PERFORMING ORGANIZATION NAME(S) AND ADDRESS(ES)
UCLA-Medicine, Hematology/Oncology
Los Angeles, California 90095-1678

E-Mail: csawyers@mednet.ucla.edu

8. PERFORMING ORGANIZATION REPORT NUMBER

9. SPONSORING / MONITORING AGENCY NAME(S) AND ADDRESS(ES)
U.S. Army Medical Research and Materiel Command
Fort Detrick, Maryland 21702-5012

10. SPONSORING / MONITORING AGENCY REPORT NUMBER

11. SUPPLEMENTARY NOTES
Original contains color plates: All DTIC reproductions will be in black and white.

12a. DISTRIBUTION / AVAILABILITY STATEMENT
Approved for Public Release; Distribution Unlimited

12b. DISTRIBUTION CODE

13. Abstract ***(Maximum 200 Words)*** *(abstract should contain no proprietary or confidential information)*

During phase II of this IDEA Award, our current focus is to study genes/pathways implicated in prostate cancer progression using transgenic mouse models. Our efforts have focused on creating transgenic models that express 1 of 4 different genes in the mouse prostate. All 4 genes were selected based on studies from our lab and others implicating these genes in human prostate cancer. These include Her-2/neu, cathepsin D, Akt and Myc. Transgenic mice for each transgene have now been created, and the phenotypes of 3 of them (cathepsin D, Akt, Myc) have been characterized. Cathepsin D and Akt mice develop prostatic intraepithelial neoplasia (PIN) only, whereas Myc mice develop PIN that progresses to invasive prostatic adenocarcinoma. In addition, we have created transgenic mice expressing the avian retrovirus receptor TVA that will allow us to introduce multiple transgenes into the prostate in a stepwise manner and to manipulate androgen levels without affecting transgene expression. We have documented successful infection with avian retroviruses expressing marker genes (GFP) and are optimizing conditions for transfer of oncogenes. We have also generated luciferase transgenic mice, which will serve as tools for imaging prostate tumor progression.

14. SUBJECT TERMS	15. NUMBER OF PAGES
Her-2/neu, cathepsin, Akt, Myc, TVA	35
	16. PRICE CODE

17. SECURITY CLASSIFICATION OF REPORT	18. SECURITY CLASSIFICATION OF THIS PAGE	19. SECURITY CLASSIFICATION OF ABSTRACT	20. LIMITATION OF ABSTRACT
Unclassified	Unclassified	Unclassified	Unlimited

Table of Contents

Introduction

Although nearly all advanced prostate cancers will respond to hormone ablation therapy using anti-androgen drugs such as leuprolide, flutamide or casodex, these tumors inevitably progress to an androgen-independent (also called hormone refractory) stage. Taxane-based chemotherapy has recently been shown to give high response rates in these patients (Petrylak et al., 1999; Smith et al., 1999), but the duration of these responses is generally short. It is clear that more insight into the molecular basis of androgen independence is needed to have a therapeutic impact. Our group has been studying this problem through the use of human prostate cancer cell lines and xenografts that undergo this transition.

The phase I portion of this proposal was entitled "Identification of genes involved in androgen independent prostate cancer progression through expression cloning." During this initial period of funding we identified two genes - the Her2/neu tyrosine kinase receptor and the cathepsin D protease - which confer androgen independent growth when introduced into androgen dependent prostate cancer cell lines (defined as the ability to grow as a subcutaneous tumor in castrate male SCID mice). These findings formed the basis of our competitive renewal (Phase II), entitled "Transgenic Models of Prostate Cancer," with the goal of generating transgenic mouse models based on genes identified through studies of our xenograft models. The original specific aims, based on the genes we had identified at the time of the competing renewal submission, were:

Aim 1 - Creation of Transgenic Mice with Constitutive Activation of the EGFR Pathway in the Prostate

We previously reported that the EGFR/Her-2 signaling pathway was upregulated in our LAPC-4 xenograft model. We have showed that overexpression of ErbB2/Her-2 is sufficient to convert prostate cells to androgen independence through ligand-independent activation of androgen receptor (AR) signaling (Craft et al., 1999). The goal of this Aim is to create transgenic mice expressing either Her-2/neu in the prostate to test the hypothesis that dysregulation of the EGFR signaling pathway is sufficient to cause prostate cancer.

Aim 2 - Further Characterization of Prostate Cancers in Cathepsin D Transgenic Mice

We isolated the cathepsin D lysosomal protease gene in a functional expression cloning screen for genes that can confer androgen-independent growth in prostate cancer cells. We have confirmed that overexpression of cathepsin D facilitates progression to androgen independence in our xenograft models and created cathepsin D transgenic mice that develop prostatic hyperplasia and prostate cancer at 1 year. The goal of this Aim is to further characterize this phenotype.

Aim 3 - Development of the TVA Retrovirus System to Introduce Multiple Transgenes into the Mouse Prostate

As the number of candidate genes implicated in prostate cancer grows, it will be necessary to create mouse models in which multiple individual mutations can be combined in the same cell. This goal has been successfully achieved in glioblastoma mouse models through the use of the TVA system (Fisher et al., 1999; Holland et al., 1998; Holland and Varmus, 1998). This model uses transgenic expression of the avian retrovirus receptor TVA in the brain to target infection of high titer, replication competent avian retroviruses expressing different oncogenes. The goal of this Aim is to create mice expressing the TVA receptor specifically in the prostate epithelium and optimize the infection of the prostate cells by avian retroviruses. This reagent will allow the introduction of oncogenes singly and in combination to create novel prostate cancer models and avoid the problem of altered transgene expression when androgen levels are manipulated.

Additional Aims developed during the past year – Creation of transgenic mice expressing Akt and c-Myc in the mouse prostate

During the past two years, we have expanded this list of genes to include Akt and c-myc, based on work from our group and others implicating both of these genes in prostate cancer progression. The results from these two additional transgenic strains are included in the progress report.

Body

Generation of mice expressing Her-2/Neu

Through our studies of human prostate cancer xenografts, we found that expression of the Her-2/neu repector tyrosine kinase was unregulated in some androgen-independent sublines when compared to isogenic controls. We also showed that overexpression of Her-2/neu was sufficient to convert androgen-dependent prostate human prostate cancer cells to androgen independence in vitro and in vivo. Finally, this gain-of-function was associated with the ability of Her-2/neu to enhance the response of the androgen receptor to limiting doses of ligand (Craft et al., 1999).

More recently, we have published our results from performing the reciprocal experiment – inhibition of the EGFR/Her-2 family of receptor tyrosine kinases in prostate cancer cells using a small molecule EGFR/Her-2 kinase inhibitor (Mellinghoff et al., 2002). The results showed that androgen-independent sublines of the LAPC4 and LAPC9 prostate cancer xenografts were more sensitive to EGFR/Her2 inhibition that isogenic androgen-dependent sublines. When castrate mice bearing androgen-independent tumors were treated with supplemental androgen, we found that the growth inhibitory effects of EGFR/Her2 inhibition were lost. These and other data from our group support a model in which prostate cells use the EGFR/Her2 pathway to send an accessory signal to the androgen receptor pathway to maximize the response to ligand. We believe the

requirement for EGFR/Her2 pathway signaling is most evident in the setting of low concentrations of androgen (as seen in the castrate state), thereby explaining the anti-tumor activity of EGFR/Her-2 inhibitors against our xenograft models in castrate animals and the "rescue" of this anti-tumor activity by androgen supplementation.

These data, together with other studies showing increased expression of Her-2/neu protein in advanced state androgen-independent cancers, provide the rationale for creating Her-2/neu transgenic mice. Because of the large size of the Her-2/neu cDNA, the initial cloning and characterization of the transgenic construct took longer than expected. However, we have now been successful in demonstrating androgen-dependent transgene expression of a construct under the control of the modified probasin promoter (ARR2/probasin) provided by Dr. Matusik at Vanderbilt (figure 1). In addition, we have now generated 2 transgene positive founder mice which have been bred and are being aged prior to sacrifice. Once we have documented transmission of the transgene to the F1 generation, we will determine the level of transgene expression in a small number of F1 males when they reach 6 weeks of age (by western blot of isolated prostate lobes, as shown below for our Akt and Myc transgenic mice). Phenotypic analysis will be conducted using standard histological methods.

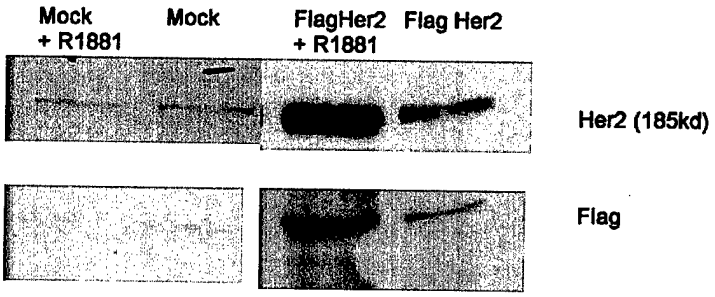

Figure 1. Androgen inducible expression of epitope-tagged Her-2/neu from the ARR2/probasin promoter. LNCaP cells were transfected with the relevant transgenic construct, then cultured in charcoal stripped serum with or without supplementation with the androgen analogue R1881. Transgene expression is documented with antibody to Her2 (top panel), the Flag epitope (bottom panel) or phosphotyrosine (not shown). Prostate lobes from transgenic mice will be screened in the same assay.

Generation of mice expressing cathepsin D

We engineered a transgenic expression construct using the basal probasin promoter (-426/+28) (previously used to generate SV40T expressing TRAMP mice) to express full length, wild-type cathepsin D in the mouse prostate. We generated 4 founder lines, demonstrated low level transgene expression by western blot in prostate lobes, and peformed histological analysis of the prostates from male mice from three different founder lines. One mouse from one founder developed a localized prostate cancer after one year of age. Although no cancers were observed in any wild-type controls, we have failed (to date) to detect any additional cancers in other transgenic lines expressing cathepsin D. Therefore, we cannot confidently ascribe the cancer phenotype in that one

mouse to cathepsin D until we have completed further analysis of more mice. The histologic features we did observe in 14 male transgene-expressing animals ranging in age from 6-18 months are detailed in table 1 in the appendix, and summarized below.

Prostate findings: The changes in the prostate are mainly seen in the anterior and dorsal lobes, which manifest primarily as an increase in glandular crowding with loss of secretions. These areas of glandular crowding likely represent foci of hyperplasia; however, there is no overt nuclear stratification, loss of nuclear polarity, pleomorphism, increased mitotic activity or invasive growth patterns to suggest prostatic adenocarcinoma. With the exception of the one mouse mentioned above who developed cancer (note: this mouse is not listed in the table), these changes are consistent with the notion that cathepsin D overexpression alone is insufficient to convert prostate cells to a neoplastic process. A major caveat is the fact that transgene expression was low. We now have data from another mouse strain (c-myc, see below) that significantly higher levels of transgene expression can be achieved using a modified probasin promoter (provided by Robert Matusik, Vanderbilt). Therefore, we have constructed a cathepsin D transgenic construct using the ARR2/probasin promoter.

Liver findings: An unexpected result in the histological analysis of the mice was the presence of steatohepatitis (defined as fatty change in the liver with inflammation) and hepatic adenomas in a significant number of the transgenic mice. In addition, these mice often had moderate splenomegaly which we attribute to pulmonary hypertension secondary the liver lesions. Three mice had clear evidence of well differentiated hepatocellular carcinomas (HCC), often appearing in a background steatohepatitis. In consultation with hepatology colleages at UCLA (Dr. Hal Yee and others), our current interpretation of these data cathepsin D is initiating an inflammatory reaction which leads to steatohepatitis. The damaged liver undergoes a process of regenerative nodular hyperplasia, which can lead to the formation of adenomatous nodules. A subset of these have the potential to become neoplastic, which we detect histologically as well differentiated hepatocellular carcinomas. A number of additional studies must be performed to explore this hypothesis further. These include: demonstration of transgene expression in the liver (which would certainly be unexpected, but it is quite possible that probasin may be expressed in a small subset of cells), molecular characterization of the adenomas and hepatocellular carcinomas, and serial analysis of multiple timepoints. Because these studies represent a diversion from the goals of our project, we plan to transfer the mice to Dr. Yee and his hepatology colleagues for further analysis.

Transgenic mice expressing constitutively active Akt develop prostatic intraepithelial neoplasia (PIN) but not prostate cancer

Work from a number of laboratories, including ours, has identified loss of function mutations or transcriptional silencing of the PTEN tumor suppressor gene as potential mechanism for prostate cancer initiation and progression (Cairns et al., 1997; Vlietstra et al., 1998; Whang et al., 1998). Homozygous deletion of PTEN causes embryonic lethality, but PTEN +/- mice develop a range of cancers, including prostate cancer. The penetrance of prostate cancer varies across genetic backgrounds and is generally low,

presumably due to more rapid development of other tumors such as lymphomas and leukemias. When PTEN +/- mice are crossed to p27 -/- mice, the incidence of prostate lesions is increased but tumors continue to develop in multiple tissues. Additional experiments are underway to define the consequences of prostate-specific deletion of PTEN by crossing mice with germline conditional PTEN knockout alleles with probasin-Cre transgenic mice (Hong Wu, UCLA, personal communication). The collective evidence from these models supports the notion that PTEN functions as a tumor suppressor gene in the prostate.

PTEN is a lipid phosphatase whose primary substrate is the phosphatidyl inositol lipid PIP3. Cells lacking PTEN have increased levels of PIP3, which functions as a second messenger to activate downstream signaling pathways by recruitment of pleckstrin homology domain (PH domain) containing proteins to the inner surface of the cell membrane. The best studied of these is Akt, a serine/threonine kinase activated by PIP3 which has oncogenic potential through regulation of a number of pathways involved in cell growth and survival (reviewed in Vivanco and Sawyers). We have generated transgenic mice expressing an active allele of Akt (Myr-Akt, which is constitutively targeted to the membrane through a myristolation sequence at the N-terminus). Our goals are: (i) to generate a transgenic mouse model caused by dyregulation of this pathway that only gives prostate cancer (in contrast to the existing PTEN knockout models) and (ii) to deterimine if constitutive Akt activation is sufficient to give a prostate cancer phenotype resembling that seen with PTEN loss (or do other PIP3-regulated pathways play a role).

As with the cathepsin D mice, the transgene was cloned into the minimal probasin promoter construct, expression was validated in cell lines, then multiple founder lines were generated and screened. In addition, we generated mice expressing myr-Akt under the control of the C3(1) promoter, which is expressed in prostate and the female breast, and has been used by Jeff Green and colleagues to develop an SV40 T Ag model of breast and prostate cancer (Maroulakou et al., 1994; Shibata et al., 1996). With both promoters we documented transgene expression in the prostate lobes by immunohistochemistry (figure 2), then examined an aged cohort of mice for pathologic findings.

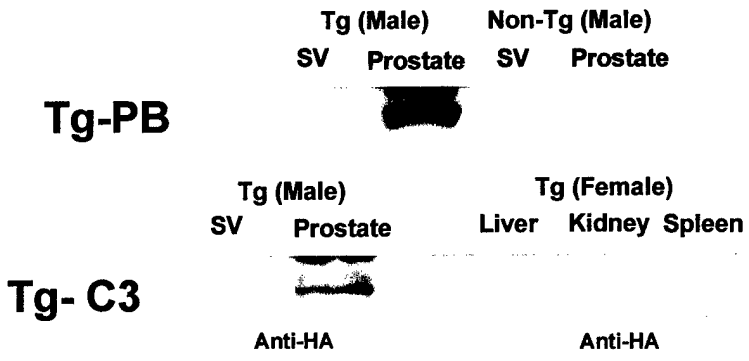

Figure 2. Expression of myr-Akt in prostate lobes of male transgenic mice. Individual lobes of the prostate (ventral, dorsal, lateral) were isolated and pooled to make protein lysates in the lanes marked "prostate." SV=seminal vesicle. The lysates in the right lanes were from wild-type controls (top panel) or transgene-positive female mice (bottom panel). Western blots were performed using an antibody to the HA epitope, which was engineered into the myr-Akt cDNA.

Prostate phenotype: Male mice from different founders of the probasin/myr-Akt mice and the C3(1)/myr-Akt mice developed preneoplastic lesions consistent with prostatic intraepithelial neoplasia (PIN). Cells in these lesions showed the following features - epithelial hyperplasia, cellular stratification, pleomorphism, nuclear and nucleolar hyperchromatism and enlargement (figure 3). Of note, these slides were reviewed as part of a prostate mouse models workshop held in October, 2001 at Jackson Labs, in conjunction with the Mouse Models of Human Cancer Consortium (MMHCC) from the NCI, and were used to help reach a consensus definition of mouse PIN. None of the animals developed prostate cancer with 12-18 months (later timepoints have not been analyzed yet).

Endometrial phenotype: Remarkably, we noted endometrial abnormalities in 8 of 16 female mice expressing the C3(1)/myr-Akt transgene, and these lesions were detected in mice ranging from age 3-14 months. The histological features (which were read in conjunction with human gynecological pathologists at UCLA) were characteristic of the human lesion called simple hyperplasia with and without atypia, which is characterized by architectural disarray (data not shown). These findings are of interest because the most penetrant phenotype in female PTEN +/- mice is complex atypical hyperplasia of the endometrium, which is a more advanced but related abnormality. Further characterization of this phenotype requires measurement of transgene expression in the uterus and more detailed analysis, which will not be pursued using the funds from this grant in order to maintain our focus on prostate cancer models.

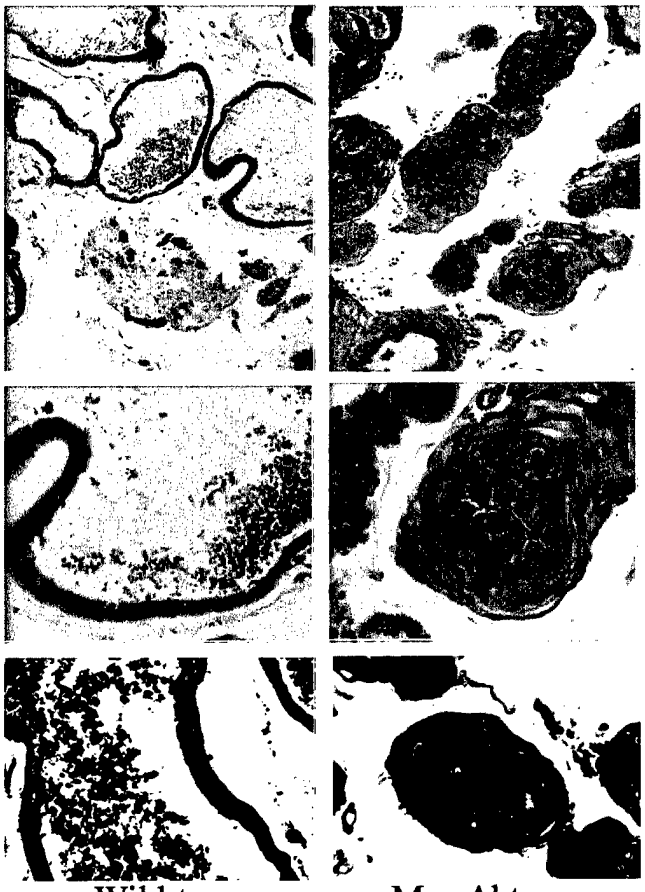

Figure 3. Prostate histology of wild-type versus Akt-transgene expressing male mice at 12 months of age. The panels show hematoxlin and eosin stained sections of mouse prostate lobes from age-matched controls (left column) and myr-Akt transgene expressing mice (right column). The lesions in the myr-Akt mice are representative examples of PIN. Similar lesions were observed in probasin/myr-Akt and in C(3)1/myr-Akt mice.

In summary, our major findings to date from the Akt transgenic mouse studies are the development of preneoplastic changes in the prostates and uteri of transgenic mice, but no overt cancers. These data, taken together with reports of Akt transgene expression in other tissues, suggest that constitutively active Akt may be involved in the early initiation stage of both these cancers but is unlikely to be sufficient to invoke invasive malignant transformation. Our next steps are: (i) to ask if higher level Akt expression (using the newer probasin promoter from Dr. Matusik, see below) gives a cancer phenotype, and (ii) to cross the mice with strains engineered to have other signaling pathway abnormalities that might complement Akt (such as p27 loss and overexpression of the Her-2/neu transgene).

Generation of mice expressing c-Myc

During our cell-based studies of transformation due to PTEN loss, we noted that PTEN null cells had increased expression and activity of the c-Myc transcription factor. In addition, c-Myc is expressed in a significant fraction of human prostate cancers and is localized to a region of chromosome 8 (8q24) that is often amplified in human prostate cancer (and even human PIN). To further investigate the potential role of c-Myc in prostate cancer, we constructed transgenic mice expressing wild-type c-Myc under the control of the simple probasin promoter (-426/+28) as well as the higher expressing ARR2/probasin promoter provided by Dr. Matusik from Vanderbilt. Multiple founders were obtained using both constructs and transgene expression was documented by western blot (figure 4). As expected, expression from the ARR2/probasin construct was significantly higher (5-10 fold) when compared to the simple probasin promoter (-426/+28) (data not shown).

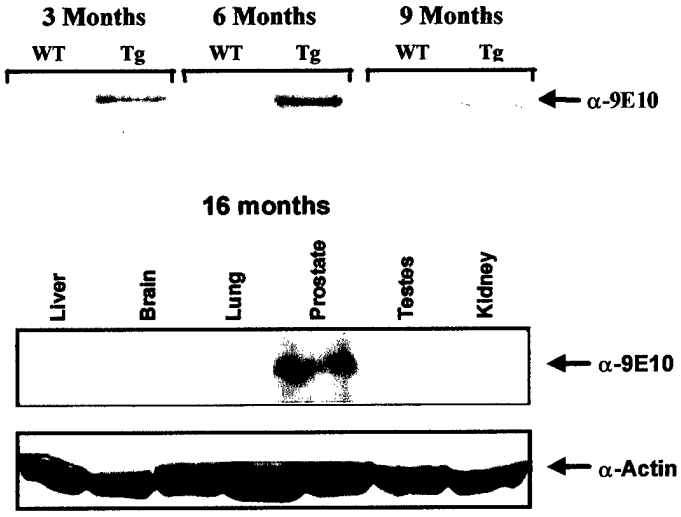

Figure 4. Prostate specific expression of the c-myc transgene in ARR2/probasin transgenic mice using the human-specific c-myc antibody 9E10.

The phenotype of transgenic Myc expression in these mice is quite striking. We first noted that all of the mice from all the founders of the ARR2/probasin Myc lines had PIN

at 3 months in the entire prostate gland. We subsequently performed detailed time course experiments that demonstrate PIN as early as 2 weeks of age, which is the earliest timepoint for initiation of transgene expression (figure 5). The penetrance of PIN is essentially 100 percent and appears to involve the entire prostate gland, raising the possibility that Myc upregulation is sufficient as a single hit to induce PIN. At six months of age all animals have invasive cancers (figure 6).

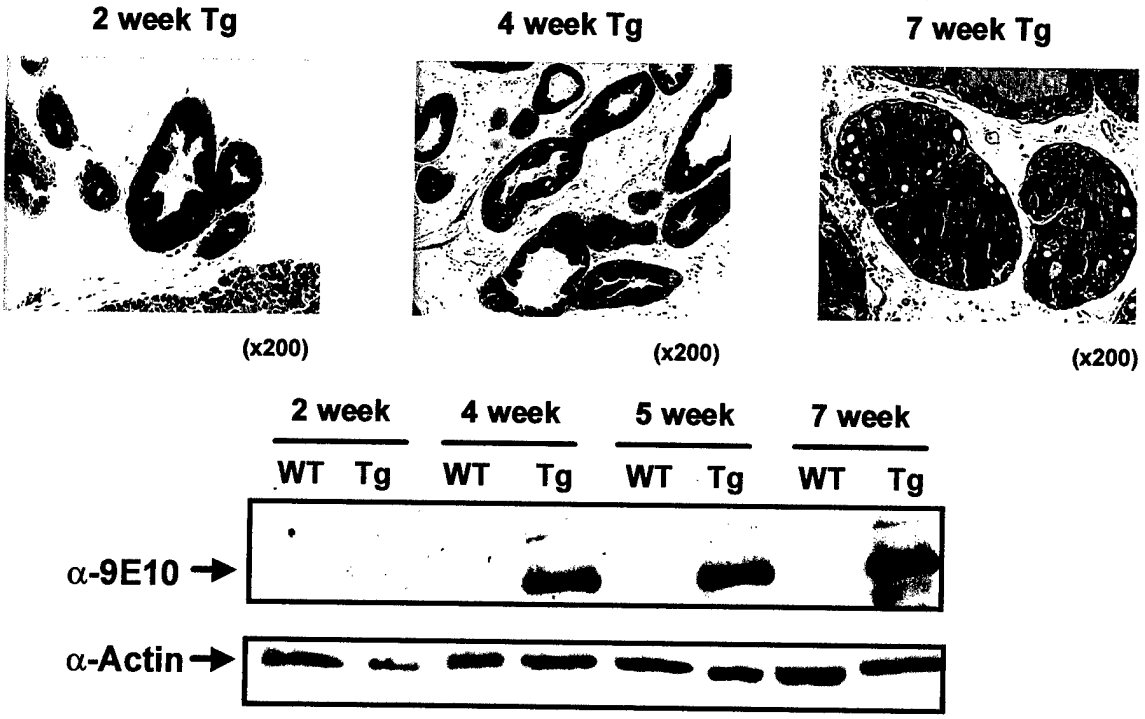

Figure 5. Transgenic expression of c-Myc induces prostatic intraepithelial neoplasia (PIN) in all mice within 2 weeks of age. The top panel shows hematoxylin and eosin stained sections of mouse prostate tissue at various time points from 2-7 weeks of age. The bottom panel shows the level of transgene expression at 2 weeks (barely detectable) and at later timepoints when expression is increased commensurate with the surge in testosterone that occurs during puberty.

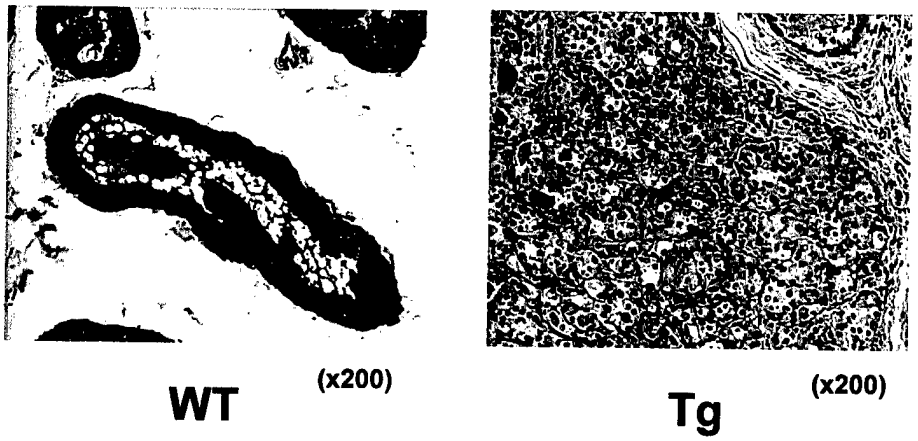

Figure 6. Transgenic expression of c-Myc induces invasive cancer in all mice by 6 months of age. The micrographs show prostate sections from 6 month old male mice expressing the ARR2/probasin Myc transgene (right panel) versus a wild-type littermate control (left panel).

In parallel with our analysis of the ARR2/probasin Myc mice, we have analyzed mice expression Myc from the probasin (-426/+28) promoter. Similar to the ARR2/probasin promoter Myc mice, the (-426/+28) promoter mice all develop PIN that progresses to invasive cancer, but with slower kinetics. Specifically, these mice all display evidence of PIN at 6 months and have invasive cancers at 12 months.

In summary, we have generated a remarkable transgenic model of prostate cancer that recapitulates the features of progression from PIN to invasive cancer seen in human disease. Of note, the tumor cells do not express the neuroendocrine marker synaptophysin, thereby distinguishing this model from the SV40 T Ag models such as TRAMP and LADY. We are currently defining the consequences of castration on PIN and tumor growth and performing genomic analysis of the lesions at different stages of progression to identify complementing events.

Generation of mice expressing the avian retrovirus receptor TVA

Recognizing the increasingly complex interplay of multiple genetic events in prostate cancer, a major goal of the competitive renewal application is to generate a model whereby multiple genes could be introduced simultaneously into the prostate gland by retroviral infection. This would avoid the time consuming process of producing individual transgenic lines for each gene of interest, then crossing multiple strains of mice. In addition, the gene of interest would be expressed under the control of the retroviral LTR promoter rather than the androgen-regulated probasin promoter, thereby allowing the effects of castration on prostate cancer growth to be distinguished from effects on transgene expression.

Toward this end, we have generated transgenic mice expressing the avian retrovirus receptor TVA under the control of the –426/+26 probasin promoter as well as the ARR2/probasin promoter. To validate the constructs, we transfected human prostate cancer cells (LNCaP) with the ARR2/probasin TVAR plasmid and infected the cells with a luciferase-expressing avian retrovirus. Using this cell line, we demonstrated that the transgenic construct made LNCaP cells permissive to avain retrovirus infection in an androgen dependent fashion (figure 7).

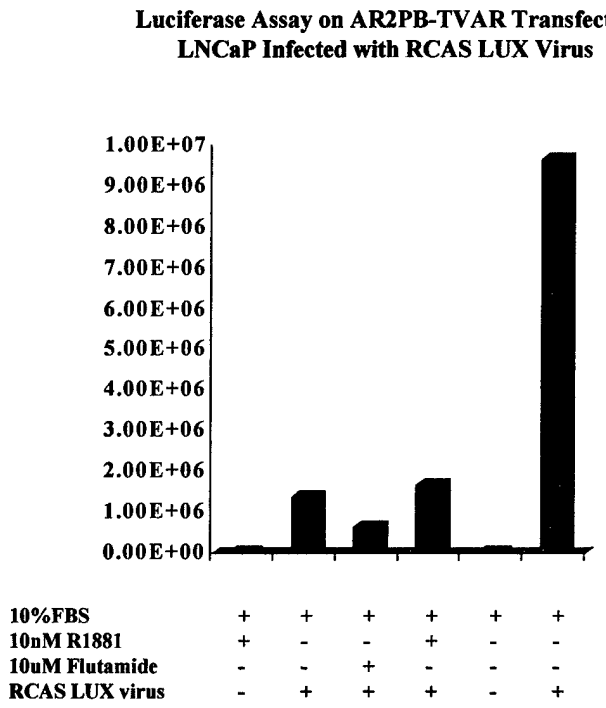

Figure 7. The ARR2/probasin TVAR transgenic construct confers androgen-inducible susceptibility to avian retrovirus infection in human prostate cancer cells. LNCaP cells were transfected with the ARR2/probasin TVAR construct, cultured in charcoal-stripped serum +/- supplemental androgen (R1881) or the androgen receptor antagonist flutamide, then infected with avain retrovirus expressing luciferase (RCAS lux). Infectivity was quantitated by luciferase assay.

Next we asked if we can infect the prostate glands of transgenic TVAR mice. Our first experiments were conducted in mice generated using the –426/+28 probasin TVAR construct, but similar experiments are in progress with the mice expressing the ARR2/probasin TVAR construct. Using avian RCAS virus expressing green fluorescent protein (GFP), we have definitive evidence of GFP expression in the prostate lobes that were injected with virus using an orthotopic injection strategy (figure 8).

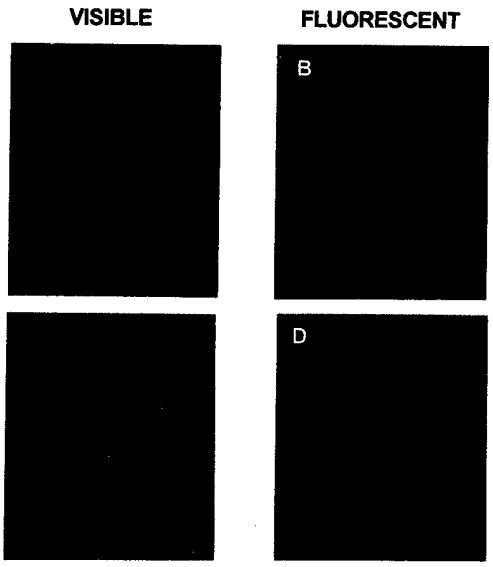

Figure 8. Injection of green fluorescent protein (GFP) expressing avian retrovirus in TVA transgenic mice. Aged matched mice were injected orthotopically with 10uL of RCAS GFP virus producing Dfl GFP cell line. Three weeks post injection, whole mounts were made of the prostates and visualized using a fluorescent microscope. Only cells containing TVA Receptor (TVAR) will be susceptible to infection and as a result glow green under fluorescent microscopy. (A and B) Dorsal-Lateral prostate from wild-type FVB mouse. No infected cells were present as can be seen in field B. (C and D) Dorsal-Lateral prostate from PB-TVAR FVB mouse. Infected cells were present as can be seen by the green cells in field D.

While this result validates the feasibility of the approach, there is much to be done to optimize gene delivery and precisely define the cell types that are infected. These studies will be accomplished using β-galactosidase expressing RCAS virus so that prostate lobes can be sectioned and stained. In addition, we are evaluating the effects of castration followed by androgen supplementation prior to virus injection in order to increase the fraction of cells in S phase (which should increase infection frequency). We are also expanding our colony of mice expressing TVAR from the ARR2/probasin promoter, and will compare the relative infection efficiency across the two strains. Finally, we are exploring different packaging envelops and vectors that offer the advantage of larger cDNA insert size. These include the helper defective avian virus BBAN as well as lentivirus backbones with ALV envelop pseudotyping (figure 9).

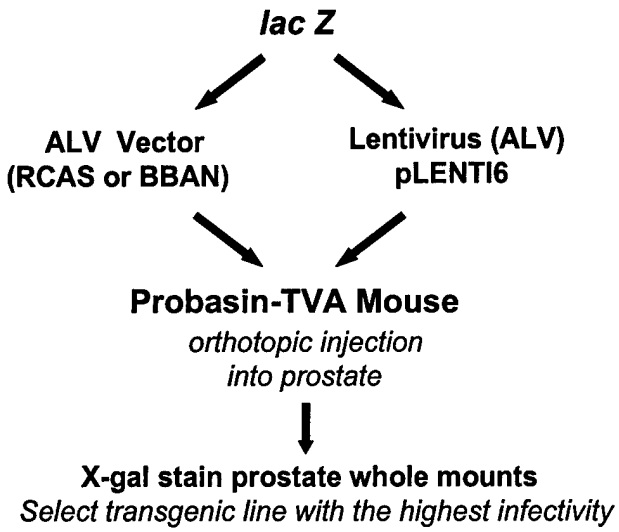

Figure 9. Flow Diagram for Determining the Efficacy of Retroviral Prostatic Injections in the Probasin-TVA Transgenic Mouse The avian leukosis virus (ALV) vector RCAS or the lentiviral vector pLENTI6 containing the *lacZ* insert were obtained. High-titer retroviral stocks will be prepared from RCAS/*lacZ* or pLENTI6/*lacZ*. pLENTI6/*lacZ* will be pseudotyped with the ALV envelope protein to allow for selective infection of prostate cells expressing the TVA receptor. Viral stocks will be delivered to the prostates of Probasin-TVA transgenic mice by orthotopic injection. Prostate whole mounts will be stained with X-gal 3 days post-injection to determine the relative infection efficiency of the multiple transgenic lines. The transgenic line displaying the highest infection efficiency will be selected for further experimentation.

Generation of luciferase expressing mice

Now that we have a number of transgenic strains with phenotypes that range from PIN (cathepsin D, Akt) to cancer (Myc), we have recognized the need to develop tools to track disease progression in a single mouse over time. After examining a number of technologies such as mouse microPET, microCT and optical imaging, we have settled on luciferase imaging as the most sensitive and user friendly. Therefore, we have generated 3 founder lines of transgenic mice expressing firefly luciferase under the control of the ARR2/probasin transgenic construct. Once we have accomplished sufficient breeding, we will validate transgene expression by intraperitoneal injection with luciferin followed by optimal imaging using the Xenogen system, which is available through the UCLA Cancer Center. Once we document successful imaging, we will cross the mice to our myc transgenics to determine the utility of this approach for following disease progression.

Key Research Accomplishments

1. Generation of Her-2/neu transgenic mice – phenotype: to be defined
2. Generation of cathepsin D transgenic mice – phenotype: PIN
3. Generation of myr-Akt transgenic mice – phenotype: PIN
4. Generation of c-myc transgenic mice – phenotype: cancer (based on feedback from a preliminary presentation of this work at a recent mouse models of cancer meeting, this strain is likely to be widely used by others)
5. Generation of TVAR transgenic mice – phenotype: susceptible to RCAS infection
6. Generation of luciferase transgenic mice – phenotype: to be defined

Reportable Outcomes

Mellinghoff I.K., Tran T., **Sawyers, C.L.** (2002) Growth inhibitory effects of the dual ErbB1/ErbB2 tyrosine kinase inhibitor PKI-166 on human prostate cancer xenografts. Cancer Research. 62:5254-5259.

Chen C.D., **Sawyers C.L.** (2002) NF-κB Activates Prostate-Specific Antigen Expression and Is Upregulated in Androgen-Independent Prostate Cancer. Mol. Cell. Biol. 22(8):2862-2870.

Conclusions

We have made considerable progress in the generation of transgenic mice that may serve as prostate cancer models. Our most significant (and perhaps surprising) accomplishment is the phenotype of the c-Myc transgenic mice, which display highly penetrant PIN and invasive adenocarcinoma, without any of the features of neuroendocrine differentiation that can be an issue with the SV40 T Ag models. In addition to optimizing the TVAR and luciferase models as tools, we will embark on crosses of mice (ie, Myc x Akt and Myc x p27 -/-) that are indicated based on oncogene cooperativity observed in vitro and genetic lesions observed in human tumors. Finally, the tumor progression in the myc mice provides an opportunity to discover complementary secondary genetic lesions using modern genomics tools such as expression microarray chips and array-based comparative genomic hybridization (CGH).

Table 1. Cathepsin D Transgenic mice pathology

TG Mouse	25	193	243	301	320
Age-months	18	16	15.5	18	17
Prostate AL	Normal	Hyperplasia	Focal Hyperplasia	Normal	Focal Hyperplasia
Prostate DL	Focal Hyperplasia	Normal	Normal	Normal	Inflammation
Prostate LL	Normal	Focal Hyperplasia	Normal	Normal	Normal
Prostate VL	Normal	Normal	Focal Hyperplasia	Normal	Normal
Seminal Vesicle	Single layer	Single layer	Single layer	N/A	N/A
Liver	N/A	Focal early Steatohepatitis and early nodule formation	Mixed Steatohepatitis and nodule formation	Adenoma; steatohepatitis	N/A

TG Mouse	322	323	379	380	381	488
Age-months	17	17	15	15	15	14
Prostate AL	Hyperplasia	Normal	Normal	Hyperplasia	Normal	Normal
Prostate DL	Hyperplasia	Normal	Normal	Hyperplasia	Normal	Focal Hyperplasia
Prostate LL	Focal Hyperplasia	Normal	Normal	Normal	Normal	Normal
Prostate VL	Focal Hyperplasia	Normal	Normal	Focal Hyperplasia	Normal	Normal
Seminal Vesicle	N/A	N/A	N/A	N/A	N/A	N/A
Liver	Adenoma; steatohepatitis with multiple areas of regeneration and nodule formation	Predominantly Microvesicular steatohepatitis	Mixed Steatohepatitis	Mixed Steatohepatitis	Focal steatosis	Mixed steatohepatitis with regeneration and nodule formation

TG mouse	876	495	496
Age-months	6	11	11
Prostate AL	Focal Hyperplasia	Focal Hyperplasia	Focal Hyperplasia
Prostate DL	Normal	Focal Hyperplasia	Normal
Prostate LL	Normal	Hyperplasia	Focal Hyperplasia
Prostate VL	Normal	Normal	Normal
Seminal Vesicle	N/A	N/A	N/A
Liver	Mixed Steatohepatitis	Adenoma; steatohepatitis	Steatohepatitis

References

Cairns, P., Okami, K., Halachmi, S., Halachmi, N., Esteller, M., Herman, J. G., Jen, J., Isaacs, W. B., Bova, G. S., and Sidransky, D. (1997). Frequent inactivation of PTEN/MMAC1 in primary prostate cancer. Cancer Res *57*, 4997-5000.

Craft, N., Shostak, Y., Carey, M., and Sawyers, C. L. (1999). A mechanism for hormone-independent prostate cancer through modulation of androgen receptor signaling by the HER-2/neu tyrosine kinase. Nat Med *5*, 280-285.

Fisher, G. H., Orsulic, S., Holland, E., Hively, W. P., Li, Y., Lewis, B. C., Williams, B. O., and Varmus, H. E. (1999). Development of a flexible and specific gene delivery system for production of murine tumor models. Oncogene *18*, 5253-5260.

Holland, E. C., Hively, W. P., DePinho, R. A., and Varmus, H. E. (1998). A constitutively active epidermal growth factor receptor cooperates with disruption of G1 cell-cycle arrest pathways to induce glioma-like lesions in mice. Genes Dev *12*, 3675-3685.

Holland, E. C., and Varmus, H. E. (1998). Basic fibroblast growth factor induces cell migration and proliferation after glia-specific gene transfer in mice. Proc Natl Acad Sci U S A *95*, 1218-1223.

Maroulakou, I. G., Anver, M., Garrett, L., and Green, J. E. (1994). Prostate and mammary adenocarcinoma in transgenic mice carrying a rat C3(1) simian virus 40 large tumor antigen fusion gene. Proc Natl Acad Sci U S A *91*, 11236-11240.

Mellinghoff, I. K., Tran, C., and Sawyers, C. L. (2002). Growth Inhibitory Effects of the Dual ErbB1/ErbB2 Tyrosine Kinase Inhibitor PKI-166 on Human Prostate Cancer Xenografts. Cancer Res *62*, 5254-5259.

Petrylak, D. P., Macarthur, R. B., O'Connor, J., Shelton, G., Judge, T., Balog, J., Pfaff, C., Bagiella, E., Heitjan, D., Fine, R., *et al.* (1999). Phase I trial of docetaxel with estramustine in androgen-independent prostate cancer. J Clin Oncol *17*, 958-967.

Shibata, M. A., Ward, J. M., Devor, D. E., Liu, M. L., and Green, J. E. (1996). Progression of prostatic intraepithelial neoplasia to invasive carcinoma in C3(1)/SV40 large T antigen transgenic mice: histopathological and molecular biological alterations. Cancer Res *56*, 4894-4903.

Smith, D. C., Esper, P., Strawderman, M., Redman, B., and Pienta, K. J. (1999). Phase II trial of oral estramustine, oral etoposide, and intravenous paclitaxel in hormone-refractory prostate cancer. J Clin Oncol *17*, 1664-1671.

Vlietstra, R. J., van Alewijk, D. C., Hermans, K. G., van Steenbrugge, G. J., and Trapman, J. (1998). Frequent inactivation of PTEN in prostate cancer cell lines and xenografts. Cancer Res *58*, 2720-2723.

Whang, Y. E., Wu, X., Suzuki, H., Reiter, R. E., Tran, C., Vessella, R. L., Said, J. W., Isaacs, W. B., and Sawyers, C. L. (1998). Inactivation of the tumor suppressor PTEN/MMAC1 in advanced human prostate cancer through loss of expression. Proc Natl Acad Sci U S A *95*, 5246-5250.

[CANCER RESEARCH 62, 5254–5259, September 15, 2002]

Growth Inhibitory Effects of the Dual ErbB1/ErbB2 Tyrosine Kinase Inhibitor PKI-166 on Human Prostate Cancer Xenografts[1]

Ingo K. Mellinghoff, Chris Tran, and Charles L. Sawyers[2]

Departments of Medicine [I. K. M., C. T., C. L. S.] and Molecular Biology Institute [C. L. S.], University of California Los Angeles, School of Medicine, Los Angeles, California, 90095

ABSTRACT

Experiments with human prostate cancer cell lines have shown that forced overexpression of the ErbB2-receptor tyrosine kinase (RTK) promotes androgen-independent growth and increases androgen receptor-transcriptional activity in a ligand-independent fashion. To investigate the relationship between ErbB-RTK signaling and androgen in genetically unmanipulated human prostate cancer, we performed biochemical and biological studies with the dual ErbB1/ErbB2 RTK inhibitor PKI-166 using human prostate cancer xenograft models with isogenic sublines reflecting the transition from androgen-dependent to androgen-independent growth. In the presence of low androgen concentrations, PKI-166 showed profound growth-inhibitory effects on tumor growth, which could be partially reversed by androgen add-back. At physiological androgen concentrations, androgen withdrawal greatly enhanced the ability of PKI-166 to retard tumor growth. The level of extracellular signal-regulated kinase activation correlated with the response to PKI-166 treatment, whereas the expression levels of ErbB1 and ErbB2 did not. These results suggest that ErbB1/ErbB2 RTKs play an important role in the biology of androgen-independent prostate cancer and provide a rationale for clinical evaluation of inhibitors targeted to this pathway.

INTRODUCTION

Carcinoma of the prostate is the most common malignancy affecting males and causes enormous morbidity and mortality in the United States and Western Europe. About one-third of men relapse after radical prostatectomy surgery because of previously undetected metastatic disease. Metastatic prostate cancer responds for a variable period of time to androgen-deprivation therapy but eventually resumes growth despite castrate levels of androgen. This state of disease, termed "androgen-independent" prostate cancer, is characterized by expression of the *AR*[3] and AR-regulated genes, suggesting that the AR pathway is reactivated in a "ligand-independent" fashion. Several mechanisms have been proposed to explain the phenomenon of AR reactivation in the setting of castrate levels of ligand. These include mutations in *AR* that alter its ligand-binding affinity, overexpression of AR because of gene amplification, and/or increased recruitment of intracellular signal transduction pathways, which activate AR through ligand-independent mechanisms (1).

ErbB RTKs have been implicated as one such pathway that may play a role in androgen-independent prostate cancer progression. Experimental support for this concept comes from the observation that: (*a*) activation of ErbB1 and/or ErbB2 RTKs by EGF or forced overexpression of ErbB2, respectively, results in androgen-independent activation of AR transcriptional activity in prostate cancer cell lines (2–4); (*b*) forced overexpression of ErbB2 promotes androgen-independent growth of prostate cancer cells (2, 3); and (*c*) androgen-independent prostate cancers express increased levels of ErbB2 receptor protein (2, 5–7). However, it is still uncertain whether ErbB1- and ErbB2-mediated signals contribute to the progression of human prostate cancer, which, unlike breast cancer (8), rarely shows amplification of *ErbB*-gene loci. Using xenograft models of human prostate cancer, we show here a striking interplay of AR and ErbB signaling pathways. Growth inhibition by the ATP site-specific ErbB1/ErbB2 RTK inhibitor PKI-166 was greatest in androgen-independent tumors, significantly augmented by simultaneous AW, and partially rescued by androgen supplementation. Growth inhibition by PKI-166 was positively correlated with the basal activation state of the ERKs ERK1/2. Our findings suggest that ErbB1/ErbB2 RTKs play an important role in the biology of human prostate cancer and may be a viable therapeutic target for novel kinase inhibitors (9).

MATERIALS AND METHODS

Reagents. The LAPC4 cell line was established from the LAPC4 human prostate cancer xenograft (10), A431 cells were kindly provided by Dr. Harvey Hershman (UCLA), and LNCaP cells were purchased from American Type Culture Collection. PKI-166 was obtained from Novartis Pharma AG, Basel, Switzerland. EGF and standard chemical reagents were obtained from Sigma. Antibodies against ErbB1 (*sc-101* and *sc-03*), ERK1/2 (*sc-94*), TGF-α (*sc-9043*), and prostate-specific antigen (*sc-7638*) were obtained from Santa Cruz Biotechnology, against ErbB2 from Oncogene Sciences (*OP-15*), against phosphotyrosine from Upstate (*4G10*), against activated ErbB1 from Chemicon (*MAb3052*), against phospho-ERK (Thr183/Tyr185) from Promega (*V8031*), and against phospho-Akt (Ser473) from Cell Signaling Technology (*Ab9271*).

Pulse-Chase Experiments and Immunoblotting. A431 cells were labeled for 12 h in methionine-free DMEM with 0.2 mCi [^{35}S]methionine/cysteine (Translabel; ICN Biomedicals) per 10-cm plate. Cells were subsequently washed three times in serum-free DMEM. Serum-free DMEM with 15 mg/liter unlabeled methionine ("chase-medium") was added to each plate in the presence or absence of 5 μM PKI-166. Ten min later 100 ng/ml EGF was added where indicated in Fig. 1*B*. Cells were lysed immediately after the third wash in serum-free DMEM (baseline sample) and at various intervals after the addition of chase-medium. Cell lysis, immunoprecipitation, SDS-PAGE-electrophoresis, autoradiography, and immunoblotting was performed following standard protocols (11). Protein concentration was determined in all of the lysates by Bio-Rad, and equal amounts of protein were loaded per lane. Quantification of immunoblot bands was performed using ImageQuant software.

Animal Experiments. SCID (C.B.-17 *Scid/Scid*) mice were bred and maintained in a laminar flow tower in a defined flora colony as described previously (12). All of the manipulations with the animals were performed in a laminar flow hood with sterile techniques following the guidelines of the UCLA Animal Research Committee. For preparation of single cell suspensions, LAPC4 (10) and LAPC9 (13) tumors continuously passaged in SCID mice were minced in serum-free Iscove's medium (Life Technologies, Inc. Grand Island, NY), washed, digested with 0.1% Pronase E (EM Science, Gibbstown, NJ), washed again, and filtered through a 200 μm nylon mesh (BioDesign Inc. of New York, Carmel, NY). The cells were plated overnight, resuspended in PrEGM, and injected with Matrigel into the right flank of SCID mice. Tumor size was determined with calipers, and mice were randomized to

Received 5/16/02; accepted 7/12/02.

The costs of publication of this article were defrayed in part by the payment of page charges. This article must therefore be hereby marked *advertisement* in accordance with 18 U.S.C. Section 1734 solely to indicate this fact.

[1] Supported by grants from the National Cancer Institute, Department of Defense, and CaPCure. C. L. S. is a Doris Duke Distinguished Clinical Scientist.

[2] To whom requests for reprints should be addressed, at 11–934 Factor Building, University of California Los Angeles-Hematology-Oncology; 10833 Le Conte Avenue, Los Angeles, CA 90095-1678. Phone: (310) 206-5585; Fax: (310) 206-8502; E-mail: csawyers@mednet.ucla.edu.

[3] The abbreviations used are: AR, androgen receptor; RTK, receptor tyrosine kinase; EGF, epidermal growth factor; ERK, extracellular signal-regulated kinase; UCLA, University of California Los Angeles; TGF, transforming growth factor; SCID, severe combined immunodeficient; AW, androgen withdrawal; MAPK, mitogen-activated protein kinase.

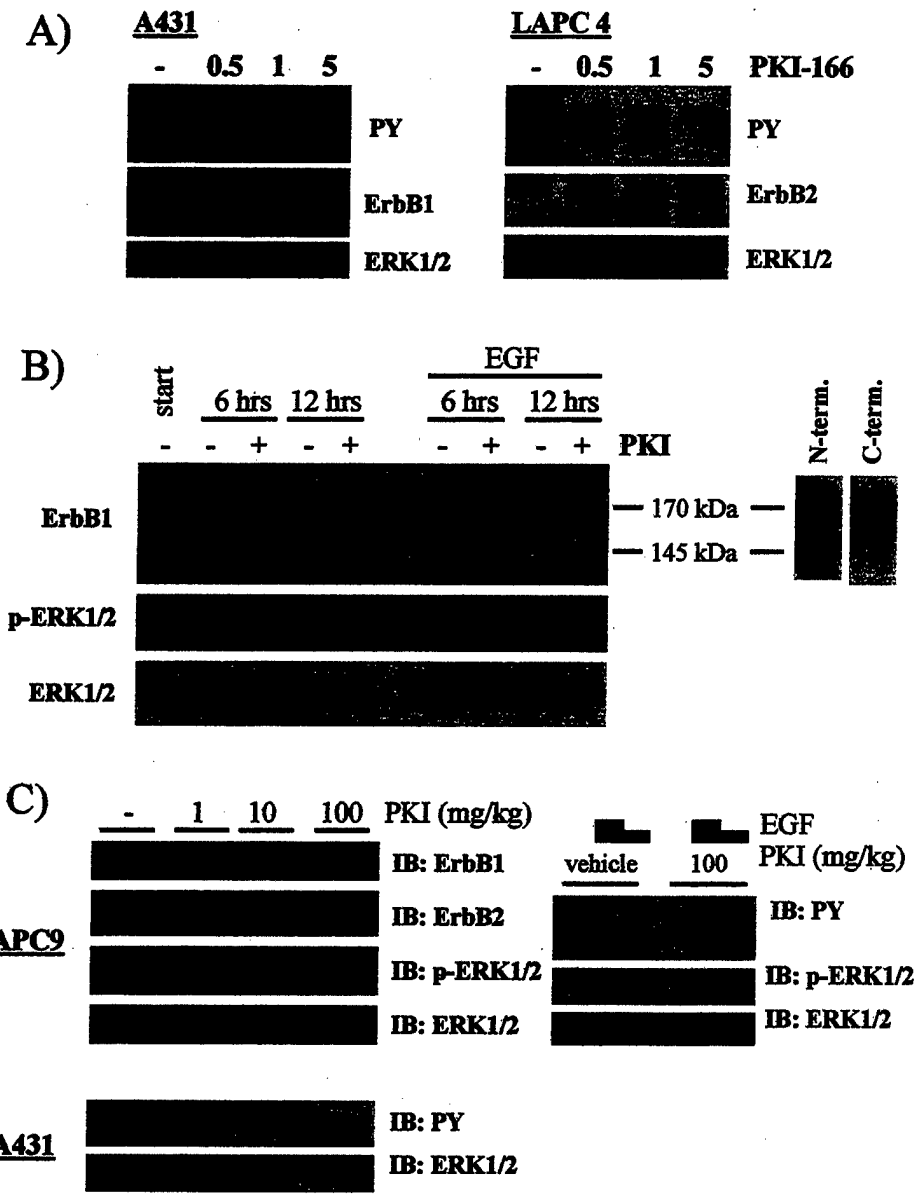

Fig. 1. PKI-166 inhibits ErbB1 and ErbB2 receptor signaling and degradation. *A*, immunoblots of A431 (*left panel*) and LAPC4 (*right panel*) cells treated for 12 h with various concentrations of PKI-166 (in μM) before stimulation with EGF (100 ng/ml) for 10 min. *B, left panel,* autoradiograph of immunoprecipitated ErbB1 (*top row*) and immunoblots (*middle and bottom row*) of lysates from A431 cells metabolically labeled for 12 h with [^{35}S]methionine and chased in the presence of PKI-166 (5 μM) and/or EGF (100 ng/ml). PKI-166 was added 10 min before EGF where indicated. *Right panel,* immunoblot of A431 cells treated with PKI-166 for 12 h using a ErbB1 antibodies directed against NH_2-terminal and COOH-terminal epitopes. *C,* immunoblots of lysates from LAPC9 (*left top panel* and *right panel*) or A431 (*left bottom panel*) xenograft tumors harvested 1 h after the fifth daily dose of PKI-166 (2 tumors per condition). The *right panel* shows lysates of LAPC9 tumors from mice injected i.p. with PBS, 0.1 mg EGF, or 0.01 mg EGF 1 h after the fifth daily dose of PKI-166. Tumors were harvested 5 min after EGF injection.

treatment groups when tumor size reached ~100 mm^3. Mean tumor volumes (in mm^3) at treatment begin was equal between groups. PKI-166 was administered daily by gavage with an 18-gauge animal feeding needle (VWR, San Dimas, CA). Testosterone pellets (Innovative Research of America) were implanted s.c. Tumor growth data are expressed as fold tumor volume compared with day 1 (Fig. 2, *A* and *C*) or as ratio between the fold increases in tumor volume for PKI-166 and vehicle treated mice ("T/C"; Figs. 2*B* and 3*B*). Statistical analyses comparing fold increases between groups were performed on the natural logarithms of the tumor volumes corrected for baseline volumes. Student's *t* test was used for comparison of two groups. ANOVA using the Tukey Studentized range method was used for multigroup comparisons.

RESULTS

PKI-166 Blocks ErbB1/ErbB2 Activity in Prostate Cancer Cells. We first examined the effects of PKI-166 on EGF-induced signal transduction through ErbB1 and ErbB2 RTKs in the human prostate cancer cell lines LAPC4 and LNCaP, both of which express the AR. The human vulvar carcinoma cell line A431, which expresses high levels of *ErbB1* because of amplification of the erbB1 locus, was used as a positive control. In A431 cells treated with EGF, immunoblotting with a phosphotyrosine antibody showed a dominant band of M_r ~170,000 representing the phosphorylated ErbB1 receptor (Fig. 1*A*). In EGF-treated LAPC-4 cells, which express considerably less ErbB1 than A431 cells but more ErbB2 (data not shown), tyrosine phosphorylation of a M_r 170,000 and a M_r 185,000 band was observed representing phosphorylated ErbB1 and ErbB2, respectively. Dose-dependent inhibition of receptor autophosphorylation was noted after pretreatment with PKI-166, with estimated IC_{50} values of 0.5 μM for ErbB1 and 5 μM for ErbB2. Similar doses of PKI-166 have been reported to inhibit phosphorylation of ErbB1 and ErbB2 RTKs but not other tyrosine or serine/threonine kinases in nonprostatic human cancer cell lines (14–16). We also noted that PKI-166 treatment resulted in a dose-dependent increase in the level of ErbB1 protein in A431 cells and ErbB2 protein in LAPC4 cells. The increase in ErbB2 expression in LAPC4 cells was apparent at 0.5 μM PKI-166, a concentration that predominantly inhibits phosphorylation of ErbB1.

Previous work has indicated that ErbB1 protein is degraded after receptor activation by ligand, raising the possibility that the increased levels of ErbB1 and ErbB2 in PKI-166-treated cells are a reflection of

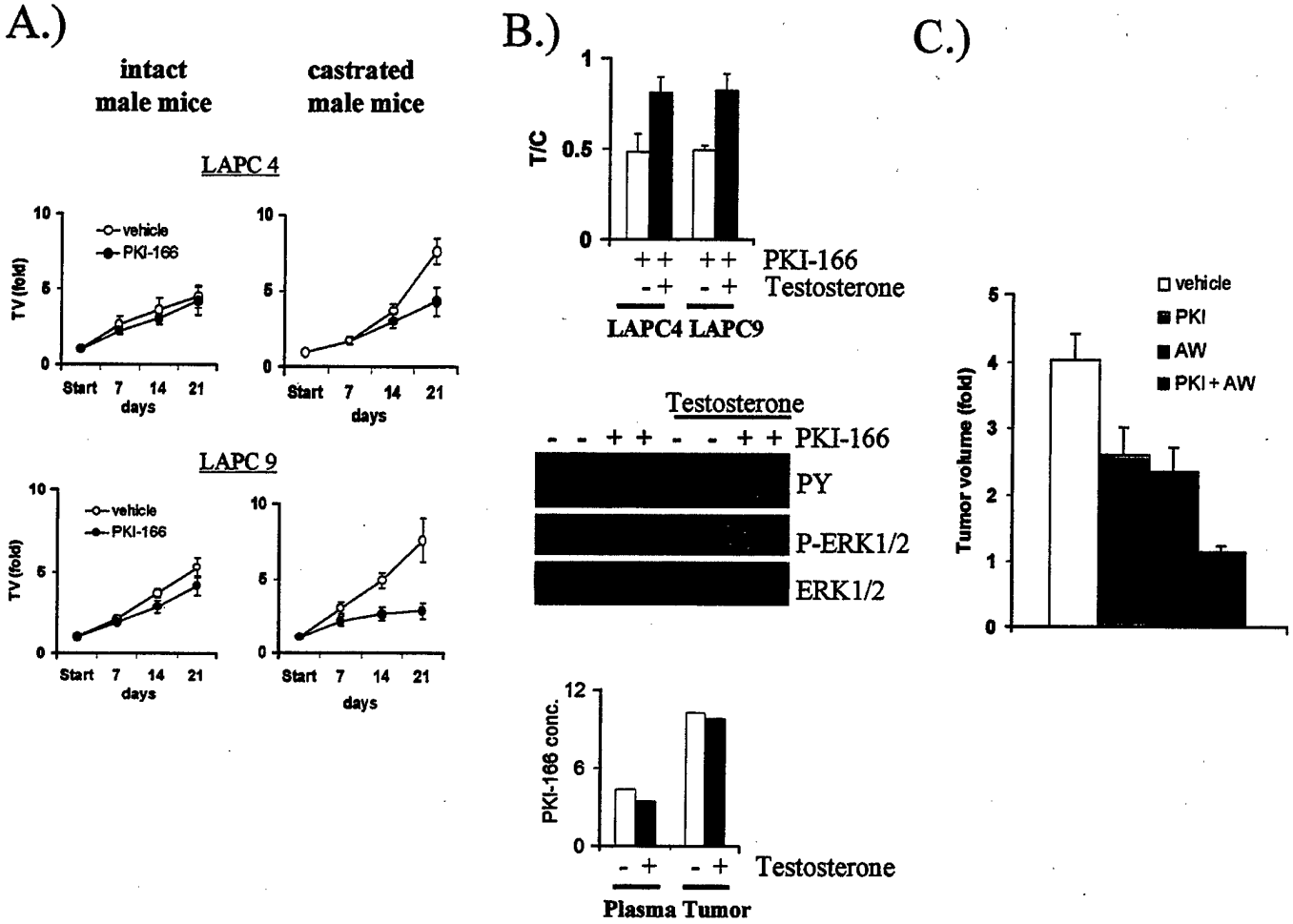

Fig. 2. Androgen modifies the growth response to PKI-166. *A*, PKI-166 inhibits the growth of human prostate cancer xenografts growing in castrated mice. Mice bearing LAPC4 or LAPC9 xenograft tumors were treated daily for 3 weeks with 100 mg/kg PKI-166 *versus* vehicle (n = 6–9 per group). Data are expressed as fold tumor volume compared with day 1; *bars*, ± SE. *B, top panel*, testosterone rescues growth inhibition by PKI-166 in castrated animals. Castrated male mice bearing androgen-independent xenografts were randomized to four treatment groups (vehicle, PKI-166, vehicle plus testosterone, and PKI plus testosterone). Data are expressed as ratio between the fold increase in tumor volume for PKI-166 treated mice and the fold increase in tumor volume for vehicle treated mice (*T/C*). Each treatment group consisted of 8–9 mice. *Middle panel*, testosterone does not impair the ability of PKI-166 to inhibit ErbB1/ErbB2 signaling. Castrated male mice bearing LAPC9 xenograft tumors were treated with PKI-166 +/− testosterone for 21 days, and EGF (0.1 mg) was administered i.p. 1 h after the last PKI-166 dose. Tumors (n = 2 per treatment condition) were harvested 5 min later. Displayed are immunoblots for PY, ERK1/2, and total ERK1/2. *Bottom panel*, testosterone does not affect PKI-166 bioavailability in mice. PKI-166 levels in plasma (μM) and LAPC9 tumors (nmol/g) were determined by reversed-phase high-performance liquid chromatography in castrated mice after 21 days of treatment with PKI-166 (100 mg/kg) +/− testosterone. Blood and tumors were collected 1 h after the last dose of PKI-166 and displayed as mean values (n = 3 per group). *C*, AW augments inhibitory effect of PKI-166 on LAPC4 xenografts in intact male mice. Surgical castration was performed on the same day as PKI-166 treatment was started. Data are expressed as fold tumor volume compared with day 1. Six mice were treated per group; *bars*, ± SE.

kinase inhibition. To determine whether pharmacologic inhibition of RTK activity delays receptor degradation, we measured the effect of PKI-166 on immunoprecipitated, [^{35}S]methionine/cysteine radiolabeled ErbB1 receptors in A431 cells (Fig. 1*B, left panel*). In the absence of PKI-166 and EGF, the receptor half-life of ErbB1 was between 6 and 12 h, consistent with the half-life of ~9 h published previously (17). Stimulation of A431 cells with EGF resulted in phosphorylation of ErbB1, as evidenced by retarded electrophoretic mobility compared with the unphosphorylated receptor, and shortening of the receptor half-life to <6 h. PKI-166 impaired the degradation of ErbB-1 receptor protein in both the presence and absence of EGF. These data support the concept that kinase activity is required for receptor degradation, consistent with prior work showing increased receptor half-life in ErbB1 alleles containing point mutations within the ErbB1 ATP-binding site (18, 19). We also noted accumulation of a lower molecular weight protein in the ErbB1 immunoprecipitates from PKI-166-treated cells. This M_r 145,000 protein was immunoprecipitated by an ErbB1 antibody directed against a cell-surface epitope but not by an antibody directed against a COOH-terminal epitope (Fig. 1*B, right panel*), indicating that it is likely to be a COOH-terminal truncation of the receptor. Similarly sized bands have been observed previously after treatment of A431 cells with the lysosomal inhibitor methylamine (17) and presumably represent an intermediate step in receptor degradation.

Because many growth factor signals are transmitted to the nucleus through ERKs (20), we also measured the effect of PKI-166 on ERK1/2 activation. At a dose that inhibits ErbB1 phosphorylation, PKI-166 completely blocked basal and EGF-induced ERK1/2 activation in A431 cells (Fig. 1*B*). Similar results were obtained in LAPC4 and LNCaP prostate cancer cells (data not shown). These data establish the biochemical activity of PKI-166 against ErbB1/ErbB2 RTKs *in vitro*, including effects on receptor autophosphorylation, receptor degradation, and additional signal transduction.

PKI-166 Blocks ErbB1/ErbB2 Signal Transduction in Tumors in Mice. We next examined the effects of PKI-166 treatment on ErbB1/ErbB2-mediated signaling *in vivo*. SCID mice bearing tumors from the human prostate cancer xenografts LAPC4 (10) and LAPC9 (13) or from the A431 cell line were treated for 5 days with 0, 1, 10, and 100 mg/kg of PKI-166, and tumor tissue was harvested 1 h after the last dose was administered. Lysates from A431 tumors displayed

constitutive phosphorylation of ErbB-1 that was inhibited by treatment of mice with 100 mg/kg PKI-166. Similar analysis of ErbB phosphorylation in prostate cancer xenografts was not informative because of low basal levels of phosphotyrosine (data not shown). However, we did observe decreased ERK1/2 activation and increased levels of total ErbB1 and ErbB2 protein in the prostate cancer xenografts from mice treated with 100 mg/kg of PKI-166, providing indirect evidence for ErbB1/ErbB2 RTK inhibition at this dose (Fig. 1*C, left panel*). To obtain direct evidence of ErbB1/ErbB2 blockade in PKI-166-treated mice, we induced receptor activation by systemic administration of EGF (21). Two different doses of EGF were injected i.p. and resulted in dose-dependent receptor phosphorylation and ERK1/2 activation in LAPC9 tumors (Fig. 1*C, right panel*). PKI-166 given p.o. at a dose of 100 mg/kg markedly blunted this activation (Fig. 1*C, right panel*). Similar results were obtained in mice bearing LAPC4 or A431 xenografts (data not shown).

PKI-166 Blocks the Growth of Prostate Cancers in Mice in an Androgen-dependent Fashion. Having defined the dose of PKI-166 required to inhibit ErbB1/ErbB2 RTKs *in vivo*, we were now able to examine the role of these RTKs in the growth of human prostate cancer. We chose the LAPC xenograft model to address this question because of its similarity to clinical prostate cancer (10) and the convenience of monitoring drug effects on s.c. tumor volumes. Tumors derived from the A431 cell line were used as a positive control and were completely growth arrested by PKI-166 (data not shown). Androgen-independent sublines of the prostate cancer xenografts grown in castrated host mice were consistently more sensitive to growth inhibition by PKI-166 than androgen-dependent sublines of the same xenograft growing in intact male ($P < 0.005$). This observation was confirmed in multiple experiments and noted in both LAPC4 and LAPC9 xenografts (Fig. 2*A*).

The trend toward enhanced activity of PKI-166 in the absence of androgen was reminiscent of our previous data showing more dramatic effects of forced ErbB2 overexpression on prostate cancer growth in castrated *versus* intact male mice (2). At that time we postulated that the major effects of ErbB1/ErbB2 pathway activation might be mediated through AR but that these effects were most relevant in the setting of low (castrate) levels of androgen. To examine this hypothesis, we asked if the suppression of growth by PKI-166 in castrated male mice could be rescued by androgen supplementation, which was administered by s.c. implantation of slow release testosterone pellets. In both LAPC4 and LAPC9 xenografts (Fig. 2*B, top panel*), androgen add-back partially rescued the growth inhibitory effects of PKI-166 ($P < 0.05$). One potential explanation for this result is that androgen impairs the ability of PKI-166 to inhibit ErbB1/ErbB2 RTKs. To examine this possibility, we treated eight castrated male mice bearing LAPC tumors with PKI-166 in the presence or absence of supplemental testosterone, and measured ErbB receptor and ERK1 activation in tumor lysates after systemic administration of EGF. Androgen supplementation did not impair the ability of PKI-166 to inhibit EGF-induced signal transduction (Fig. 2*B, middle panel*) nor did androgen affect the bioavailability of PKI-166 as shown by similar mean plasma and tumor drug levels in castrated and androgen-supplemented mice (Fig. 2*B, bottom panel*). These data indicate that the rescue of PKI-166-induced growth suppression by androgen supplementation cannot be explained by a failure of PKI-166 to inhibit its target. Rather, our findings suggest that ErbB1/ErbB2 signaling is not required for prostate cancer growth when androgen is present at high levels.

If a threshold level of circulating androgen exists below which ErbB1/ErbB2 RTKs are required for prostate cancer growth, acute AW by surgical castration should increase the growth-inhibitory effects of PKI-166. To test this hypothesis, we randomized intact male SCID mice bearing the LAPC4 xenograft to four treatment groups. Compared with vehicle-treated mice, AW by surgical castration slowed the growth of LAPC4 tumors ($P < 0.05$), as expected (10). Growth inhibition by PKI-166 given at 100 mg/kg daily did not reach statistical significance. However, the combination of PKI-166 with AW resulted in nearly complete growth suppression (Fig. 2*C*). The difference between the combined treatment group and any of the other three treatment groups was highly statistically significant ($P < 0.001$).

Sensitivity to Growth Inhibition by PKI-166 Is Correlated with ERK Activation. The LAPC-4 and LAPC-9 xenografts have been passaged in mice over multiple generations, and various androgen-dependent and androgen-independent subclones derived from the original parental lines have been maintained independently. In the course of these studies we noted that subclones derived from the same parental line occasionally displayed differences in their sensitivity to PKI-166. These sublines provide an opportunity, within an isogenic system, to examine variables in the ErbB1/ErbB2 signaling pathway that might determine response to ErbB1/ErbB2 inhibition. To address this question, we performed biochemical analysis on six LAPC xenograft clones, of which four were grown in intact male mice (clones 1 and 2 for both LAPC 4 and LAPC 9) and two in castrated male mice (clones 3 for both LAPC 4 and LAPC 9). We examined not only the expression levels of the direct PKI-166 targets ErbB1 and ErbB2, but also the activation state of the Ras/MAPK and phosphatidylinositol 3′-kinase/Akt-pathways. Both pathways are considered central effectors of the ErbB signaling network (20) and have been implicated in the progression of human prostate cancer (3, 22–24). Expression of the ErbB-1 ligand TGF-α was included in the analysis because of its suggested role as an autocrine growth factor in androgen-independent prostate cancer (25). To be able to correlate for each subline the expression of these biochemical parameters with the growth response to PKI-166, we quantified the relevant immunoblot bands (Fig. 3*A*) by densitometry. Despite differences in the magnitude of ERK1/2-activation between the LAPC4 and LAPC9 xenograft models, we found within each model a positive correlation between the degree of growth-inhibition by PKI-166 and the level of ERK1/2-activation (Fig. 3*B*). No such correlation was found for expression levels of ErbB1, ErbB2, TGF-α, or activation level of Akt. Whereas the number of available sublines for each xenograft was not sufficient to perform a multivariate analysis, our results in an isogenic system suggest that expression levels of ErbB-1 or ErbB-2 are not sufficient to determine sensitivity to PKI-166 and are consistent with studies using the ErbB-1 inhibitor ZD1839 (26) or the anti-ErbB-2 monoclonal antibody Mab 4D5 (27).

We also noted that androgen-independent tumors (clones 3) showed increased activation of ERK1/2 when compared with tumors grown in intact male mice (Fig. 3*A*). This observation was confirmed by serial analysis of androgen-dependent LAPC4 xenografts at various times postcastration during the evolution to androgen independence (Fig. 3*B*). This data are consistent with results of immunohistochemical analyses of human prostate cancer specimens using phosphospecific antibodies to ERK1/2 (28).

DISCUSSION

In conclusion, our study shows that ErbB1/ErbB2 RTKs contribute to the growth of human prostate cancer and that this contribution is greatest when levels of androgen are limiting. The nature of the interaction between AR pathway and ErbB1/ErbB2 RTKs remains to be defined. It is conceivable that ErbB-RTKs provide growth and survival signals for prostate cancer cells, which are completely independent of AR and only biologically relevant under the selective pressure of androgen deprivation. Alternatively, ErbB-RTKs might

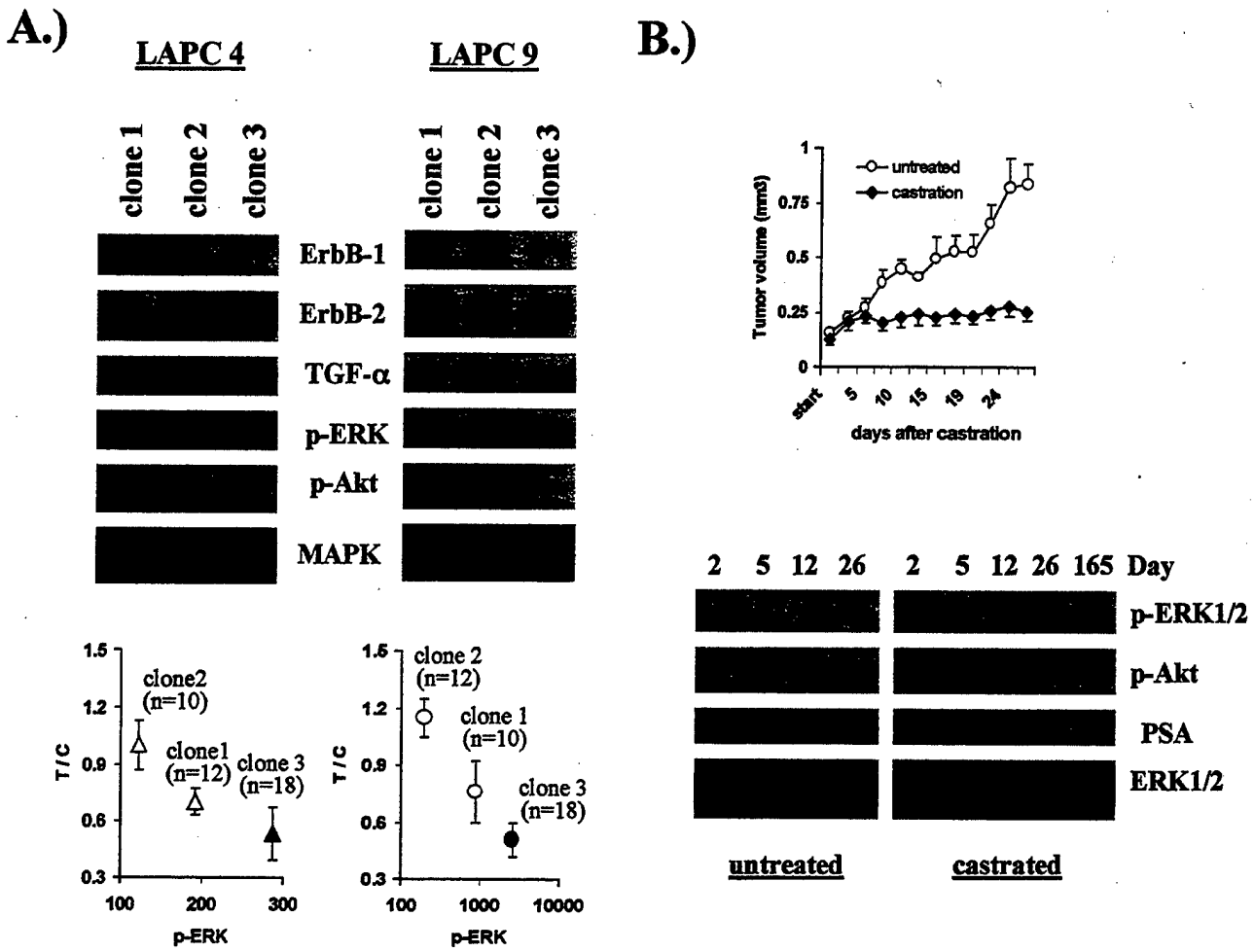

Fig. 3. Activity of p-ERK correlates with growth-inhibition by PKI-166 *in vivo* and is increased in androgen-independent tumors. *A, top panel,* immunoblot of tumor lysates from six different LAPC sublines; *bottom panel,* correlation between growth inhibition by PKI-166 and levels of activated ERK for six LAPC clones. Immunoblot bands were quantified by densitometry, and the absolute value under the peak was plotted on the X-axis. The Y-axis shows the ratio between the fold increase in tumor volume for PKI-166 treated mice and the fold increase in tumor volume for vehicle treated mice (*T/C*). *Open symbols* represent xenograft clones grown in intact mice; *closed symbols* represent xenograft clones growing in castrated animals. *B,* effect of castration on p-ERK levels in LAPC4 xenograft tumors harvested at various time points after castration; *bars,* ±SE.

promote prostate cancer growth through ligand-independent activation of AR (2, 3). MAPKs, the primary effectors of the ErbB/Ras/Raf signaling pathway, have been suggested to link growth factor receptors and steroid hormone receptors, possibly by direct phosphorylation of the latter (29). In that context, our observation that increased ERK1/2 activation is positively correlated with response to ErbB1/ErbB2 pathway inhibition is particularly intriguing and warrants additional investigation.

A growing number of small molecule inhibitors of ErbB1 and/or ErbB2 are making their way into clinical trials and show slightly different potencies in relative inhibition of ErbB1 *versus* ErbB2 RTKs (9). Because these compounds appear to have therapeutic effects in subsets of patients, the question of which kinase is important for targeting, ErbB1 or ErbB2, is frequently raised. The dose of PKI-166 (100 mg/kg) used in most of our experiments inhibited both ErbB1 and ErbB2 RTKs, as evidenced by biochemical studies on tumor lysates, comparison of drug levels in mice with *in vitro* drug concentrations, and recent data from other mouse models of cancer treated with PKI-166 (15). Interestingly, the ErbB-2 RTK monoclonal antibody Herceptin failed to inhibit the growth of androgen-independent sublines of the CWR22 human prostate cancer xenograft model (30). Whereas this difference may reflect the use of different cell lines, it raises the possibility that inhibition of the ErbB-1 RTK is required to halt androgen-independent growth.

Despite the difficulty in dissecting the relative contribution of individual ErbB-receptor family members in naturally arising tumors, our data provide rationale for testing ErbB1/2-RTK inhibitors in clinical trials of human prostate cancer. It may also offer some guidance for the design of such studies. Whereas most current trials study the effects of ErbB-inhibitors in patients who failed hormonal therapy, our data suggest a role for combining ErbB-RTK inhibition with AW for patients with early-stage disease. Our findings also raise the possibility that the activation state of the Ras/MAPK pathway in clinical specimens might serve as a biomarker to identify tumors that "depend" on this pathway and may be more likely to respond to treatment with ErbB1/ErbB2 inhibitors.

ACKNOWLEDGMENTS

We thank Drs. Elisabeth Buchdunger and Peter Traxler (Novartis Pharma AG) for providing PKI-166, Drs. Josef Brueggen and Robert Cozens (Novartis Pharma AG) for determination of PKI-166 concentrations, Dr. Elliot Landaw (UCLA) for statistical analyses, Randy Chen for technical assistance, and Phuong Huynh for assistance in preparation of the manuscript.

REFERENCES

1. Grossmann, M. E., Huang, H., and Tindall, D. J. Androgen receptor signaling in androgen-refractory prostate cancer. J. Natl. Cancer Inst., *93:* 1687–1697, 2001.

2. Craft, N., Shostak, Y., Carey, M., and Sawyers, C. L. A mechanism for hormone-independent prostate cancer through modulation of androgen receptor signaling by the HER-2/neu tyrosine kinase. Nat. Med., *5:* 280–285, 1999.
3. Yeh, S., Lin, H. K., Kang, H. Y., Thin, T. H., Lin, M. F., and Chang, C. From HER2/Neu signal cascade to androgen receptor and its coactivators: a novel pathway by induction of androgen target genes through MAP kinase in prostate cancer cells. Proc. Natl. Acad. Sci. USA, *96:* 5458–5463, 1999.
4. Culig, Z., Hobisch, A., Cronauer, M. V., Radmayr, C., Trapman, J., Hittmair, A., Bartsch, G., and Klocker, H. Androgen receptor activation in prostatic tumor cell lines by insulin- like growth factor-I, keratinocyte growth factor, and epidermal growth factor. Cancer Res., *54:* 5474–5478, 1994.
5. Signoretti, S., Montironi, R., Manola, J., Altimari, A., Tam, C., Bubley, G., Balk, S., Thomas, G., Kaplan, I., Hlatky, L., Hahnfeldt, P., Kantoff, P., and Loda, M. Her-2-neu expression and progression toward androgen independence in human prostate cancer. J. Natl. Cancer Inst., *92:* 1918–1925, 2000.
6. Osman, I., Scher, H. I., Drobnjak, M., Verbel, D., Morris, M., Agus, D., Ross, J. S., and Cordon-Cardo, C. HER-2/neu (p185neu) protein expression in the natural or treated history of prostate cancer. Clin. Cancer Res., *7:* 2643–2647, 2001.
7. Shi, Y., Brands, F. H., Chatterjee, S., Feng, A. C., Groshen, S., Schewe, J., Lieskovsky, G., and Cote, R. J. Her-2/neu expression in prostate cancer: high level of expression associated with exposure to hormone therapy and androgen independent disease. J. Urol., *166:* 1514–1519, 2001.
8. Slamon, D. J., Clark, G. M., Wong, S. G., Levin, W. J., Ullrich, A., and McGuire, W. L. Human breast cancer: correlation of relapse and survival with amplification of the HER-2/neu oncogene. Science (Wash. DC), *235:* 177–182, 1987.
9. Mendelsohn, J. The epidermal growth factor receptor as a target for cancer therapy. Endocr. Relat. Cancer, *8:* 3–9, 2001.
10. Klein, K. A., Reiter, R. E., Redula, J., Moradi, H., Zhu, X. L., Brothman, A. R., Lamb, D. J., Marcelli, M., Belldegrun, A., Witte, O. N., and Sawyers, C. L. Progression of metastatic human prostate cancer to androgen independence in immunodeficient SCID mice. Nat. Med., *3:* 402–408, 1997.
11. Daub, H., Wallasch, C., Lankenau, A., Herrlich, A., and Ullrich, A. Signal characteristics of G protein-transactivated EGF receptor. EMBO J., *16:* 7032–7044, 1997.
12. Chackal-Roy, M., Niemeyer, C., Moore, M., and Zetter, B. R. Stimulation of human prostatic carcinoma cell growth by factors present in human bone marrow. J. Clin. Investig., *84:* 43–50, 1989.
13. Craft, N., Chhor, C., Tran, C., Belldegrun, A., DeKernion, J., Witte, O. N., Said, J., Reiter, R. E., and Sawyers, C. L. Evidence for clonal outgrowth of androgen-independent prostate cancer cells from androgen-dependent tumors through a two-step process. Cancer Res., *59:* 5030–5036, 1999.
14. Bruns, C. J., Solorzano, C. C., Harbison, M. T., Ozawa, S., Tsan, R., Fan, D., Abbruzzese, J., Traxler, P., Buchdunger, E., Radinsky, R., and Fidler, I. J. Blockade of the epidermal growth factor receptor signaling by a novel tyrosine kinase inhibitor leads to apoptosis of endothelial cells and therapy of human pancreatic carcinoma. Cancer Res., *60:* 2926–2935, 2000.
15. Brandt, R., Wong, A. M., and Hynes, N. E. Mammary glands reconstituted with Neu/ErbB2 transformed HC11 cells provide a novel orthotopic tumor model for testing anti-cancer agents. Oncogene, *20:* 5459–5465, 2001.
16. Scheving, L. A., Stevenson, M. C., Taylormoore, J. M., Traxler, P., and Russell, W. E. Integral role of the EGF receptor in HGF-mediated hepatocyte proliferation. Biochem. Biophys. Res. Commun., *290:* 197–203, 2002.
17. Stoscheck, C. M., and Carpenter, G. Down regulation of epidermal growth factor receptors: direct demonstration of receptor degradation in human fibroblasts. J. Cell Biol., *98:* 1048–1053, 1984.
18. Honegger, A. M., Dull, T. J., Felder, S., Van Obberghen, E., Bellot, F., Szapary, D., Schmidt, A., Ullrich, A., and Schlessinger, J. Point mutation at the ATP binding site of EGF receptor abolishes protein-tyrosine kinase activity and alters cellular routing. Cell, *51:* 199–209, 1987.
19. Chen, W. S., Lazar, C. S., Poenie, M., Tsien, R. Y., Gill, G. N., and Rosenfeld, M. G. Requirement for intrinsic protein tyrosine kinase in the immediate and late actions of the EGF receptor. Nature (Lond.), *328:* 820–823, 1987.
20. Yarden, Y., and Sliwkowski, M. X. Untangling the ErbB signalling network. Nat. Rev. Mol. Cell. Biol., *2:* 127–137, 2001.
21. Donaldson, R. W., and Cohen, S. Epidermal growth factor stimulates tyrosine phosphorylation in the neonatal mouse: association of a M(r) 55, 000 substrate with the receptor. Proc. Natl. Acad. Sci. USA, *89:* 8477–8481, 1992.
22. Gioeli, D., Zecevic, M., and Weber, M. J. Immunostaining for activated extracellular signal-regulated kinases in cells and tissues. Methods Enzymol., *332:* 343–353, 2001.
23. Wen, Y., Hu, M. C., Makino, K., Spohn, B., Bartholomeusz, G., Yan, D. H., and Hung, M. C. HER-2/neu promotes androgen-independent survival and growth of prostate cancer cells through the Akt pathway. Cancer Res., *60:* 6841–6845, 2000.
24. Malik, S. N., Brattain, M., Ghosh, P. M., Troyer, D. A., Prihoda, T., Bedolla, R., and Kreisberg, J. I. Immunohistochemical demonstration of phospho-akt in high Gleason grade prostate cancer. Clin. Cancer Res., *8:* 1168–1171, 2002.
25. Scher, H. I., Sarkis, A., Reuter, V., Cohen, D., Netto, G., Petrylak, D., Lianes, P., Fuks, Z., Mendelsohn, J., and Cordon-Cardo, C. Changing pattern of expression of the epidermal growth factor receptor and transforming growth factor α in the progression of prostatic neoplasms. Clin. Cancer Res., *1:* 545–550, 1995.
26. Moasser, M. M., Basso, A., Averbuch, S. D., and Rosen, N. The tyrosine kinase inhibitor ZD1839 ("Iressa") inhibits HER2-driven signaling and suppresses the growth of HER2-overexpressing tumor cells. Cancer Res., *61:* 7184–7188, 2001.
27. Lane, H. A., Beuvink, I., Motoyama, A. B., Daly, J. M., Neve, R. M., and Hynes, N. E. ErbB2 potentiates breast tumor proliferation through modulation of p27(Kip1)-Cdk2 complex formation: receptor overexpression does not determine growth dependency. Mol. Cell. Biol., *20:* 3210–3223, 2000.
28. Gioeli, D., Mandell, J. W., Petroni, G. R., Frierson, H. F., Jr., and Weber, M. J. Activation of mitogen-activated protein kinase associated with prostate cancer progression. Cancer Res., *59:* 279–284, 1999.
29. Kato, S., Endoh, H., Masuhiro, Y., Kitamoto, T., Uchiyama, S., Sasaki, H., Masushige, S., Gotoh, Y., Nishida, E., Kawashima, H., and *et al.* Activation of the estrogen receptor through phosphorylation by mitogen-activated protein kinase. Science (Wash. DC), *270:* 1491–1494, 1995.
30. Agus, D. B., Scher, H. I., Higgins, B., Fox, W. D., Heller, G., Fazzari, M., Cordon-Cardo, C., and Golde, D. W. Response of prostate cancer to anti-Her-2/neu antibody in androgen-dependent and -independent human xenograft models. Cancer Res., *59:* 4761–4764, 1999.

MOLECULAR AND CELLULAR BIOLOGY, Apr. 2002, p. 2862–2870
0270-7306/02/$04.00+0 DOI: 10.1128/MCB.22.8.2862–2870.2002

Vol. 22, No. 8

NF-κB Activates Prostate-Specific Antigen Expression and Is Upregulated in Androgen-Independent Prostate Cancer

Charlie D. Chen and Charles L. Sawyers*

Division of Hematology/Oncology, Department of Medicine, University of California at Los Angeles, Los Angeles, California 90095-1678

Received 12 December 2001/Accepted 19 January 2002

The transcription factor NF-κB regulates gene expression involved in cell growth and survival and has been implicated in progression of hormone-independent breast cancer. By expressing a dominant-active form of mitogen-activated protein kinase kinase kinase 1, by exposure to tumor necrosis factor alpha, or by overexpression of p50/p65, we show that NF-κB activates a transcription regulatory element of the prostate-specific antigen (PSA)-encoding gene, a marker for prostate cancer development, treatment, and progression. By DNase I footprinting, we identified four NF-κB binding sites in the PSA core enhancer. We also demonstrate that androgen-independent prostate cancer xenografts have higher constitutive NF-κB binding activity than their androgen-dependent counterparts. These results suggest a role of NF-κB in prostate cancer progression.

Prostate cancer begins as an androgen-dependent (AD) tumor and regresses in response to androgen ablation therapy. This therapy eventually fails, and the tumor progresses despite castrate levels of androgen. This stage of the disease is referred to as androgen-independent (AI) or hormone-refractory prostate cancer. The prostate-specific antigen (PSA) level in serum is a clinical marker for prostate cancer progression and effectiveness of treatment. Rising PSA levels typically signal progression from androgen dependence to androgen independence. Biochemical and genetic analyses have identified two regulatory regions responsible for androgen-regulated, tissue-specific PSA expression—the proximal promoter containing a core TATA box and an enhancer region located approximately 4.2 kb upstream of the transcription start site (7, 19, 33). We have used these regions as tools with which to identify molecular mechanisms responsible for PSA expression at castrate levels of androgen to gain insight into mechanisms of prostate cancer progression (2, 9).

The NF-κB/Rel genes encode a family of heterodimeric transcription factors that share a 300-amino-acid Rel homology domain (RHD) (16, 26). Classical NF-κB is a heterodimer composed of a 50-kDa (p50) subunit and a 65-kDa (p65 or RelA) subunit and was discovered as a κ-immunoglobulin enhancer DNA binding protein (38). c-Rel, another member of

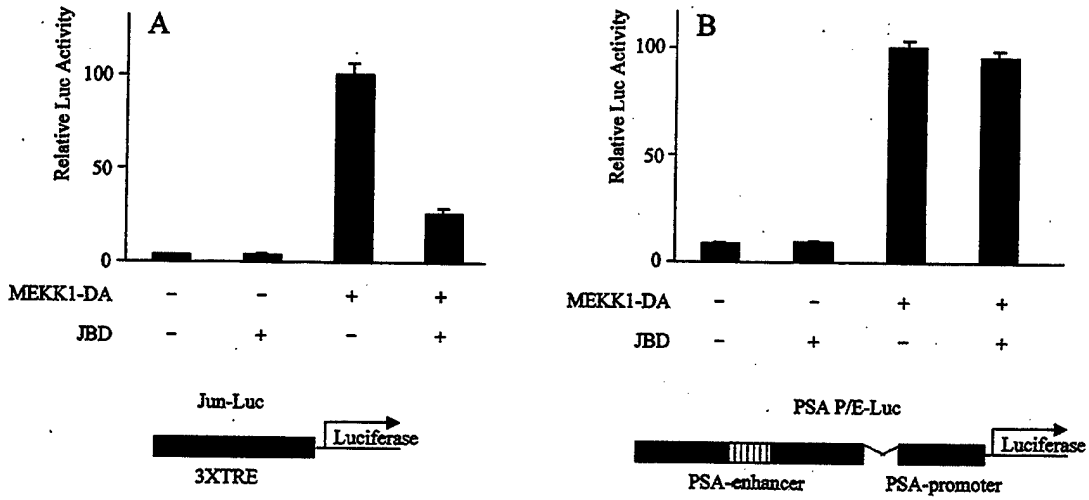

FIG. 1. JBD does not inhibit MEKK1-mediated activation of PSA. LNCaP cells were transfected with empty vector pcDNA3, JBD (500 ng), MEKK1-DA (400 ng), or JBD with MEKK1-DA, together with the reporter construct driven either by a Jun-responsive element (Jun-Luc; 200 ng) (A) or by PSA-P/E–Luc (200 ng) (B). Luciferase activity was measured 2 days after transfection and normalized by transfection efficiency, which was determined by GFP cotransfection. The data shown represent three experiments.

* Correspondent author. Mailing address: 11-934 Factor Building, UCLA-Hematology-Oncology, 10833 Le Conte Ave., Los Angeles, CA 90095-1678. Phone: (310) 206-5585. Fax: (310) 206-8502. E-mail: csawyers@mednet.ucla.edu.

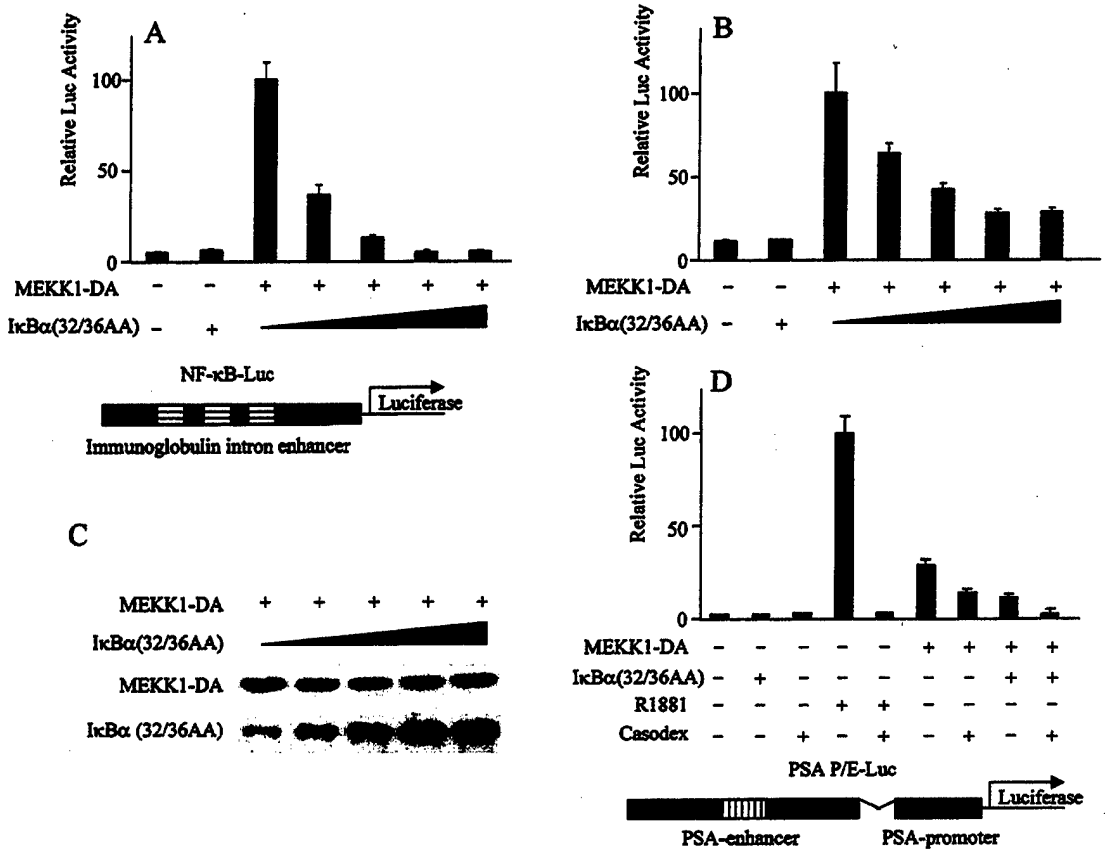

FIG. 2. Dominant-active IκBα mutant inhibits MEKK1-mediated activation of PSA. LNCaP cells were transfected with empty vector pcDNA3, the mutant form IκBα(32/36AA) (800 ng), MEKK1-DA (300 ng), or MEKK1-DA with increasing amounts (100, 200, 400, and 800 ng) of the mutant form IκBα(32/36AA), together with the reporter construct driven either by an NF-κB-responsive element (NF-κB–Luc; 200 ng) (A) or by PSA-P/E–Luc (200 ng) (B and D). (C) Lysates from the transfected cells were examined for MEKK1-DA expression. Bicalutamide was used as indicated in the experiment whose results are shown in panel D. Luciferase activity was measured 2 days after transfection and normalized by transfection efficiency, which was determined by GFP cotransfection. The data shown represent three experiments.

this family, was originally identified as a proto-oncogene. The activity of these proteins is regulated primarily through post-translational modification. In unstimulated cells, the NF-κB/Rel proteins are sequestered in the cytoplasm by association with inhibitory proteins, termed inhibitor of NF-κB (IκBα and IκBβ). Upon phosphorylation by IκB kinases (IKKs), IκB is modified by ubiquitination and degraded, allowing NF-κB to translocate into the nucleus and activate target gene transcription (16).

Breast cancer studies have proposed a role for NF-κB in the progression of hormone-dependent cancers to hormone independence. Constitutive activation of NF-κB was found in estrogen receptor (ER)-negative breast cancer cell lines and poorly differentiated primary tumors (29). Progression of the rat mammary carcinoma cell line RM22-F5 from an ER-positive, nonmalignant phenotype to an ER-negative, malignant phenotype was accompanied by constitutive activation of NF-κB (29). The current data on prostate cancer are less certain. In the AI prostate cell lines PC-3 and DU-145, the DNA binding activity of NF-κB is constitutively activated whereas the androgen-sensitive prostate cancer cell line LNCaP has a low level of NF-κB binding activity (31). However, PC-3 and DU-145 do not express androgen receptor (AR) and PSA; therefore, the relevance of this finding to clinical AI prostate cancer progression is not clear. In a different set of studies, the RelA subunit of NF-κB was shown to inhibit AR function by competing for the coactivator CREB binding protein (CBP) (1, 32). This result suggests that NF-κB may play a negative role in AI progression since AR activation (not suppression) is associated with prostate cancer progression.

We have examined this issue in two xenograft models of AD-to-AI prostate cancer progression in which AR expression and PSA expression are retained (8, 23). We showed previously that mitogen-activated protein kinase kinase kinase 1 (MEKK1) activates PSA expression in prostate cancer cells (2). This activation is only partially abolished by the AR inhibitor bicalutamide (Casodex), suggesting that pathways other than AR may be involved in this activation. MEKK1 can activate Jun N-terminal kinase (JNK) or IκB kinase (IKK), resulting in activation of the AP-1 or NF-κB transcription factor complex, respectively. In this report, we demonstrate that NF-κB, but not AP-1, is required for MEKK1 to fully activate PSA transcription. We also identify previously unrecognized NF-κB binding sites in the PSA enhancer and show that progression to

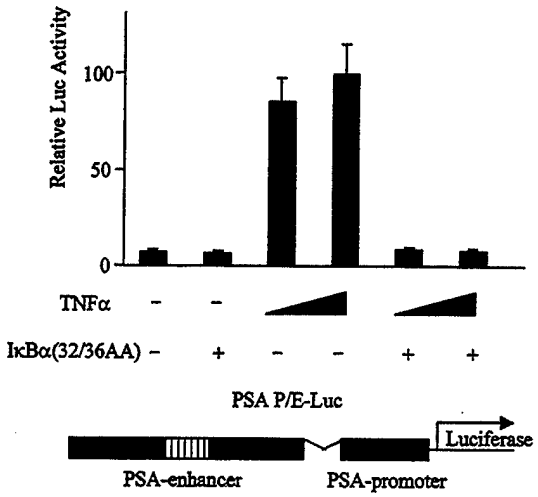

FIG. 3. TNF-α activates PSA expression through the NF-κB pathway. LNCaP cells were transfected with the reporter construct PSA-P/E–Luc (200 ng) with or without the mutant form IκBα(32/36AA) (800 ng) as indicated. After transfection, cells were treated with or without TNF-α (10 or 50 ng/ml) as indicated. Luciferase activity was measured 2 days after transfection and normalized to *Renilla* luciferase. The data shown represent two experiments.

AI is associated with increased constitutive NF-κB binding activity in both xenograft models.

MATERIALS AND METHODS

Cell culture and xenograft. The human prostate cancer cell lines LNCaP and DU145 were obtained from the American Type Culture Collection and maintained in RPMI 1640 medium supplemented with 10% fetal bovine serum (FBS). For phorbol 12-myristate 13-acetate (PMA) and tumor necrosis factor alpha (TNF-α) treatment, LNCaP cells were grown in the presence of 10% FBS overnight and subsequently in the absence of serum for 2 days. The serum-starved LNCaP cells were challenged with 5% charcoal-stripped FBS with or without PMA (10 ng/ml) or TNF-α (50 ng/ml) overnight, and the media were subjected to enzyme-linked immunosorbent assay (ELISA; American Qualex) to determine PSA expression. The LAPC-4 and LAPC-9 xenograft models were established as previously described (9, 23) and maintained subcutaneously in mice. Progression to AI was modeled by castration of mice bearing AD tumors.

Plasmids. The cDNA of MEKK1-DA (MEKK1 dominant active) was subcloned into pcDNA3 as previously described (2). MEKK1-DA is a truncated form of MEKK1 in which the N-terminal 351 amino acids were deleted. The PSA promoter enhancer luciferase reporter (PSA-P/E–Luc) was constructed by inserting a 600-bp fragment of the PSA promoter and a 2.4-kb enhancer sequence upstream of luciferase (pSE) as previously described (2, 9, 33). Constructs containing mutations in the NF-κB binding sites on PSA-P/E–Luc were kindly provided by Michael Carey (University of California at Los Angeles) and were prepared as previously described (19). The IκBα mutant contains amino acid substitutions of serines 32 and 36 to alanine. Plasmids encoding the IκBα mutant, p50, p65, and c-Rel were kindly provided by Genhong Cheng (University of California at Los Angeles).

Transfection. LNCaP or DU145 cells were plated at 40 to 50% confluency and transfected 1 day later in accordance with the manufacturer's instructions using TFX-50 (Promega) for LNCaP and Lipofectamine plus (Promega) for DU145. To minimize interference from androgen, transfected cells were maintained in RPMI 1640 medium supplemented with 5% charcoal-stripped serum. Two days after transfection, cells were harvested and the luciferase activity of the reporter constructs was measured with a luciferase assay kit or a dual luciferase assay kit (Promega). Luciferase activity was normalized to the percentage of green fluorescent protein (GFP)-positive cells in transfections that included pcDNA3-enhanced GFP or to *Renilla* luciferase when the pRL-TK plasmid was used as the normalization control.

DNase I footprinting. Probes were created by PCR with the reporter plasmid PSA-P/E–Luc, which contains the PSA core enhancer, as a template. The 3′ primers were ACCAGCTCAATCAGTCAC, CATGTTCACATTAGTACACC, AACCTGAGATTAGGAATCC, and TGAGAGAGATATCATCTTGC. The common 5′ primer was CGTTGAGACTGTCCTGCAG. The 3′ primers were end labeled by T4 polymerase kinase with [γ-^{32}P]ATP, and each 3′ primer was combined with the common 5′ primer to PCR amplify DNA probe for footprinting. The binding reactions for DNase footprinting were as previously described (13). The DNA was precipitated and resolved on a 6 to 8% polyacrylamide–7 M urea sequencing gel. Recombinant human p50 was purchased from Promega.

EMSAs. Concentrated nuclear extracts for electrophoretic mobility shift assays (EMSAs) were prepared as previously described (6). Nuclear extracts were diluted in buffer containing 2 mM EDTA, 25 mM HEPES (pH 7.5), 150 mM NaCl, 1% Triton X-100, and 10% glycerol. The wild-type and mutant double-strand probes were purchased from Operon. They are GCCATGGGGGGATC CCCGAAGTCC and GCCATGGGCCGATCCCCGAAGTCC. The probes were end labeled by T4 polymerase kinase with [γ-^{32}P]ATP. Diluted nuclear extracts were incubated with the indicated probe in the same buffer as for DNase I footprinting (13), except that glycerol was added to a final concentration of 1%. Antibodies against NF-κB p50 (SC-114 X), p65 (SC-372-G), and AR (SC-816) were also incubated in supershift experiments. After 1 h of incubation, the reaction mixture was resolved in a 6% native polyacrylamide electrophoresis gel in buffer containing 0.5× Tris-borate-EDTA and 1% glycerol.

Western blot analysis. Nuclear extracts and cytoplasmic fractions of xenograft tumors were prepared as previously described (6). Western blot analysis was performed in accordance with standard procedures (35). The antibodies used in this study were SC-1643 against IκBα, SC-945 against IκBβ, SC-372-G against NF-κB p65, SC-1190 against NF-κB p50 (Santa Cruz Biotechnology), and AC-15 against β-actin (Sigma).

RESULTS

NF-κB, but not AP-1, is required for MEKK1-mediated activation of the PSA-P/E. Previously, we demonstrated that a constitutively active form of MEKK1 (MEKK1-DA) induces AR-independent activation of the PSA promoter-enhancer (PSA-P/E) (2). To identify mechanisms responsible for this activation, we used dominant-negative mutant forms to examine downstream pathways of MEKK1.

An AP-1 binding site was previously identified in the PSA enhancer by sequence inspection (36). Because MEKK1 activates AP-1 through JNK, we asked if JNK is required for MEKK1-mediated induction of PSA. LNCaP cells were cotransfected with MEKK1-DA and JBD, a truncated form of JIP-1 that selectively inhibits JNK (11). In a titration experiment, the minimal dose of plasmid MEKK1-DA required to fully activate the PSA-P/E was defined (data not shown). Transfected cells were maintained in 5% charcoal-stripped serum to minimize interference from androgen. As expected, MEKK1 stimulated transcription of a c-Jun-responsive element and the activation was inhibited by JBD (Fig. 1A). MEKK1-DA activated the PSA-P/E, but this activation could not be blocked by JBD (Fig. 1B). This result is consistent with our previous finding that JBD does not impair the effect of MEKK1 on prostate cancer cell survival (2) and suggests that AP-1 is not involved in MEKK1-mediated activation of PSA.

Another target of MEKK1 is IKK. MEKK1 activates IKK, which phosphorylates IκB, leading to NF-κB activation. To determine if NF-κB is involved in MEKK1-mediated activation of PSA, LNCaP cells were transfected with MEKK1-DA and a dominant-active form of IκBα containing alanine substitutions at serines 32 and 36. These mutations prevent phosphorylation by IKK, thereby preventing NF-κB translocation to the nucleus to activate transcription. Cotransfection of the mutant IκBα

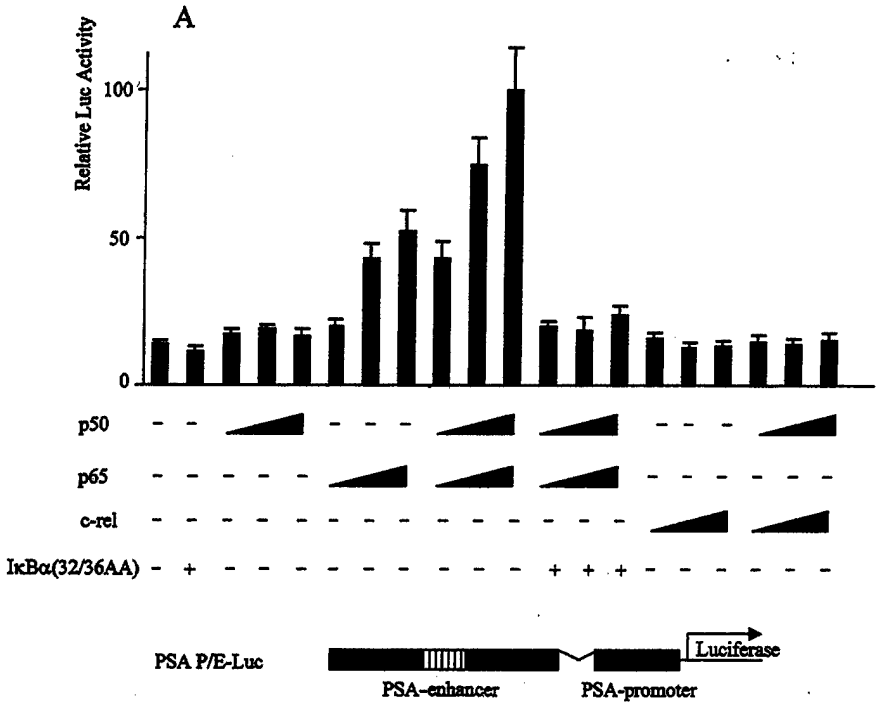

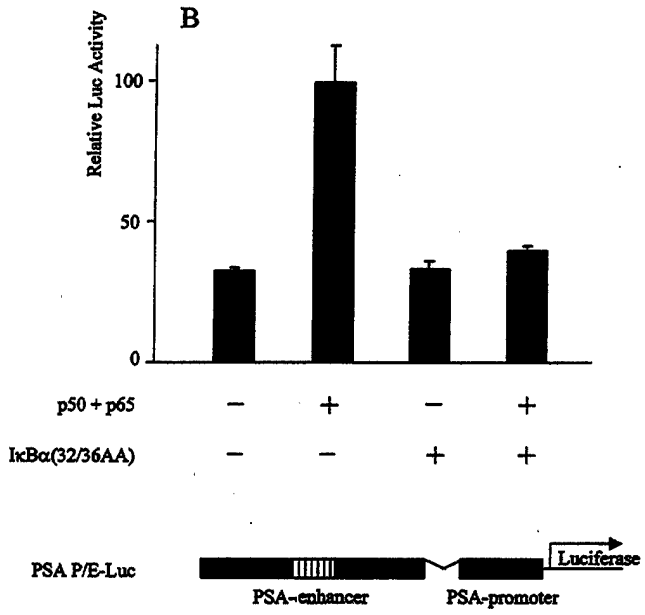

FIG. 4. Overexpression of NF-κB activated PSA expression, and the activation was abolished by mutant IκBα. (A) LNCaP cells were transfected with the reporter construct PSA-P/E–Luc (200 ng) with increasing amounts of human p50 (p50) (25, 50, and 100 ng), human p65 (p65) (25, 50, and 100 ng), a combination of p50 and p65, c-Rel (25, 50, and 100 ng), or a combination of p50 and c-Rel and with or without the mutant form IκBα(32/36AA) (800 ng) as indicated. (B) DU145 cells were cotransfected with the reporter construct PSA-P/C–Luc (200 ng) and p50 (50 ng) and p65 (50 ng) and with or without the mutant form IκBα(32/36AA) (800 ng) as indicated. Luciferase activity was measured 2 days after transfection and normalized to *Renilla* luciferase. The data shown represent two experiments.

blocked the effect of MEKK-DA on an NF-κB-responsive element (Fig. 2A) and on the PSA-P/E (Fig. 2B) in a dose-dependent manner. The expression level of MEKK-DA did not change when the mutant IκBα was cotransfected (Fig. 2C). While large doses of the mutant IκBα completely abolished the effect of MEKK1-DA on the NF-κB-responsive element (Fig. 2A), the maximal effect on the PSA-P/E was a reduction by 65% (Fig. 2B). However, PSA activation was completely abolished when both bicalutamide and the mutant IκBα were used (Fig. 2D), consistent with our previous observation that MEKK1-DA also activates AR (2).

NF-κB activates the PSA-P/E. If NF-κB is required for transcriptional activation of PSA by MEKK1-DA, we reasoned

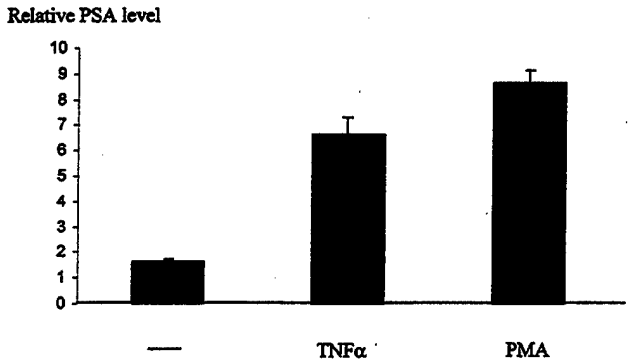

FIG. 5. TNF-α and PMA induce endogenous PSA expression. Serum-starved LNCaP cells were grown in 5% charcoal-stripped FBS with or without TNF-α (50 nM) or PMA (10 ng/ml) overnight, and the media were subjected to ELISA to determine PSA expression.

A

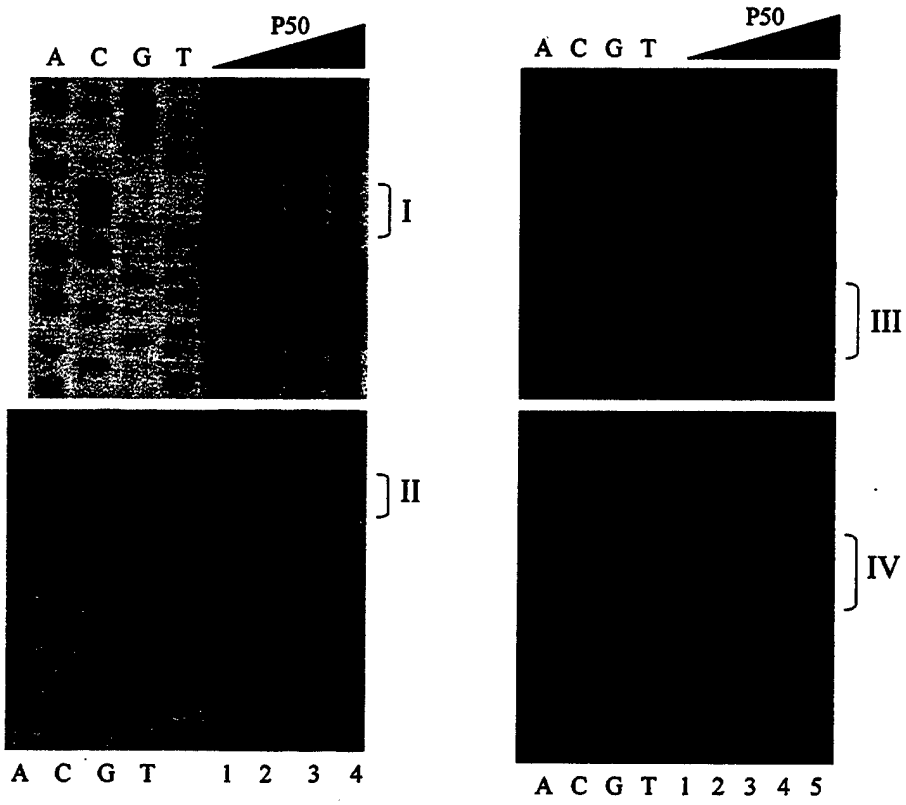

B

```
catgttcaca ttagtacacc ttgcccccc caaatcttgt
agggtgacca gagcagtcta ggtggatgct gtgcagaagg
ggtttgtgcc actggtgaga aacctgagat taggaatcct
caatcttata ctgggacaac ttgcaaacct gctcagcctt
tgtctctgat gaagatatta tcttcatgat cttggattga
aaacagacct actctggagg aacatattgt atcgattgtc
cttgacagta aacaaatctg ttgtaagaga cattatcttt
attatctagg acagtaagca agcctggatc tgagagagat
atcatcttgc aaggatgcct gctttacaaa catccttgaa
acaacaatcc agaaaaaaaa aggtgttgct gtctttgctc
agaagacaca cagatacgtg acagaaccat ggagaattgc
ctcccaacgc tgttcagcca gagccttcca cccttgtctg
caggacagtc tcaacg
```

NF-KB consensus sequence	**GGGRNNYYCC**	
Protected sites	**GGGGGGggCa**	I (reversed)
	GGGGTTTgtg	II
	GGGACAaCtt	III
	GGtGTTgCtg	IV

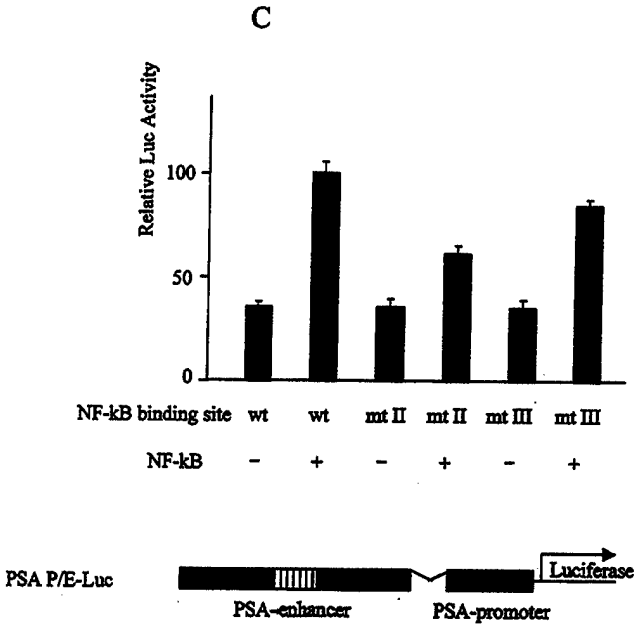

FIG. 6. Identification of NF-κB binding sites in PSA core enhancer. (A) Increasing amounts of recombinant human p50 protein (0, 0.5, 1.0, 2.0, and 4.0 gel shift units in lanes 1, 2, 3, 4, and 5, respectively) were incubated with a ^{32}P-labeled enhancer fragment, from −4366 to −3824, to detect footprints. The sites identified are designated I, II, III, and IV in sequence order. Sequencing ladders are included alongside the footprints to localize the protected sites. The order of binding affinity was I > II > III > IV. (B) Sequence of the PSA core enhancer. Footprinted regions are underlined and compiled below the consensus. The sequence of site I is reversed. (C) Wild-type (wt) or mutant PSA-P/E–Luc was cotransfected with p50 and p65 into LNCaP cells. Luciferase activity was measured 2 days after transfection and normalized by transfection efficiency, which was determined by GFP cotransfection. The data shown represent three experiments. Sites II and III were mutated to CCGGTTTGTG and ACGGAGTACT, respectively.

that other signals that lead to activation of NF-κB may also activate the PSA-P/E. Indeed, TNF-α, a cytokine that activates NF-κB, was sufficient to activate PSA-P/E transcription in LNCaP cells, and this activation was completely blocked by the mutant IκBα (Fig. 3). To provide more direct evidence that NF-κB plays a regulatory role in PSA transcription, we asked if NF-κB is sufficient to increase PSA-P/E transcriptional activity. Overexpression of p50, the NF-κB subunit without a transcriptional activation domain, did not activate the PSA-P/E (Fig. 4A). However, overexpression of p65, or the combination of p50 and p65, did activate the PSA-P/E and this activation was abolished by cotransfection of the mutant IκBα (Fig. 4A). It is noteworthy that c-Rel, another member of the p65 family, did not activate the PSA-P/E (Fig. 4A). These results indicate that NF-κB is sufficient to activate the PSA-P/E in the absence of androgen and suggests that this activation may be specific to the classical p50/p65 NF-κB complex. We performed a similar experiment with DU145 cells, a prostate cancer cell line that does not express AR. Cotransfection of p50/p65 activated the PSA-P/E reporter in the absence of AR, and this activation was blocked by the mutant IκBα (Fig. 4B). While the levels of NF-κB-induced PSA reporter induction are lower than those achieved by transfection of AR and addition of androgen (data not shown), these data demonstrate that NF-κB is sufficient to activate PSA expression independently of AR.

TNF-α and PMA stimulate endogenous PSA expression. To determine whether NF-κB activates endogenous PSA expression, LNCaP cells were challenged with two commonly used NF-κB-inducing agents, TNF-α and PMA, both of which are known to activate NF-κB in LNCaP cells (20, 28). This approach, rather than cotransfection of p50/p65 plasmids, was necessary to ensure NF-κB activation in a large population of cells (because of low transfection efficiency). Cells were maintained in RPMI 1640 medium without serum for 2 days to deplete PSA and then challenged with TNF-α or PMA in 5% charcoal-stripped FBS. PSA expression was determined by ELISA (26, 37). Both TNF-α and PMA stimulated PSA production (Fig. 5), suggesting that NF-κB activation alone is sufficient to stimulate PSA expression.

NF-κB directly binds the PSA enhancer. To determine whether activation of PSA transcription by NF-κB was a direct or indirect effect, DNase footprinting analysis was performed. We analyzed a core enhancer between −4366 and −3824 because this region was previously shown to be important for androgen-induced PSA expression (7, 19, 33). The ^{32}P-labeled PSA core enhancer was incubated with recombinant p50 protein, and the reaction mixture was subjected to DNase I digestion. p50 protected four regions in the PSA core enhancer with the following order of binding affinity: I > II > IV > III (Fig. 6A). One-half of a gel shift unit (defined as the amount of p50 required to shift 0.38 pmol of the NF-κB oligonucleotide) completely protected site I from DNase digestion, and one gel shift unit greatly reduced DNase digestion of site II. The four protected sequences (Fig. 6B) in the PSA core enhancer resemble a κB consensus sequence (GGGRNNYYCC) (26), and the order of NF-κB binding affinity is consistent with the prediction from a comparative analysis (42). This result indicates that NF-κB can directly bind to the PSA enhancer.

To determine the functional role of these sites, we examined the effect of NF-κB on promoters containing mutations in sites II and III. We chose mutations in these two sites because they have intermediate DNA binding affinity (Fig. 6B). Both mutations abolished the footprinting of p50, as expected (data not shown). In addition, both mutations showed reduced activation by NF-κB (Fig. 6C).

Increased NF-κB binding activity in AI prostate cancer. To determine if NF-κB activity correlates with ligand-independent PSA expression during AI prostate cancer progression, we measured NF-κB binding activity in the LAPC-4 and LAPC-9 prostate cancer xenograft models by EMSA. A strong band shift was detected when 2 μg of nuclear extract from LAPC-4 AI tumor tissue was used (Fig. 7A, lane 8). The band shift was also seen when smaller quantities of nuclear extracts from LAPC-4 AI tumor tissue were used (Fig. 7A, lanes 6 and 7). However, nuclear extracts from LAPC-4 AD tumor tissue formed barely detectable shifted complexes, even at high concentrations (Fig. 7A, lanes 3 to 5). This result suggests that AI tumor tissue has a higher constitutive NF-κB binding activity than its AD counterpart. Similar results were observed in the LAPC-9 xenograft model, although the basal level of NF-κB activation in LAPC-9 AD is already elevated (Fig. 7A, lanes 9 to 14).

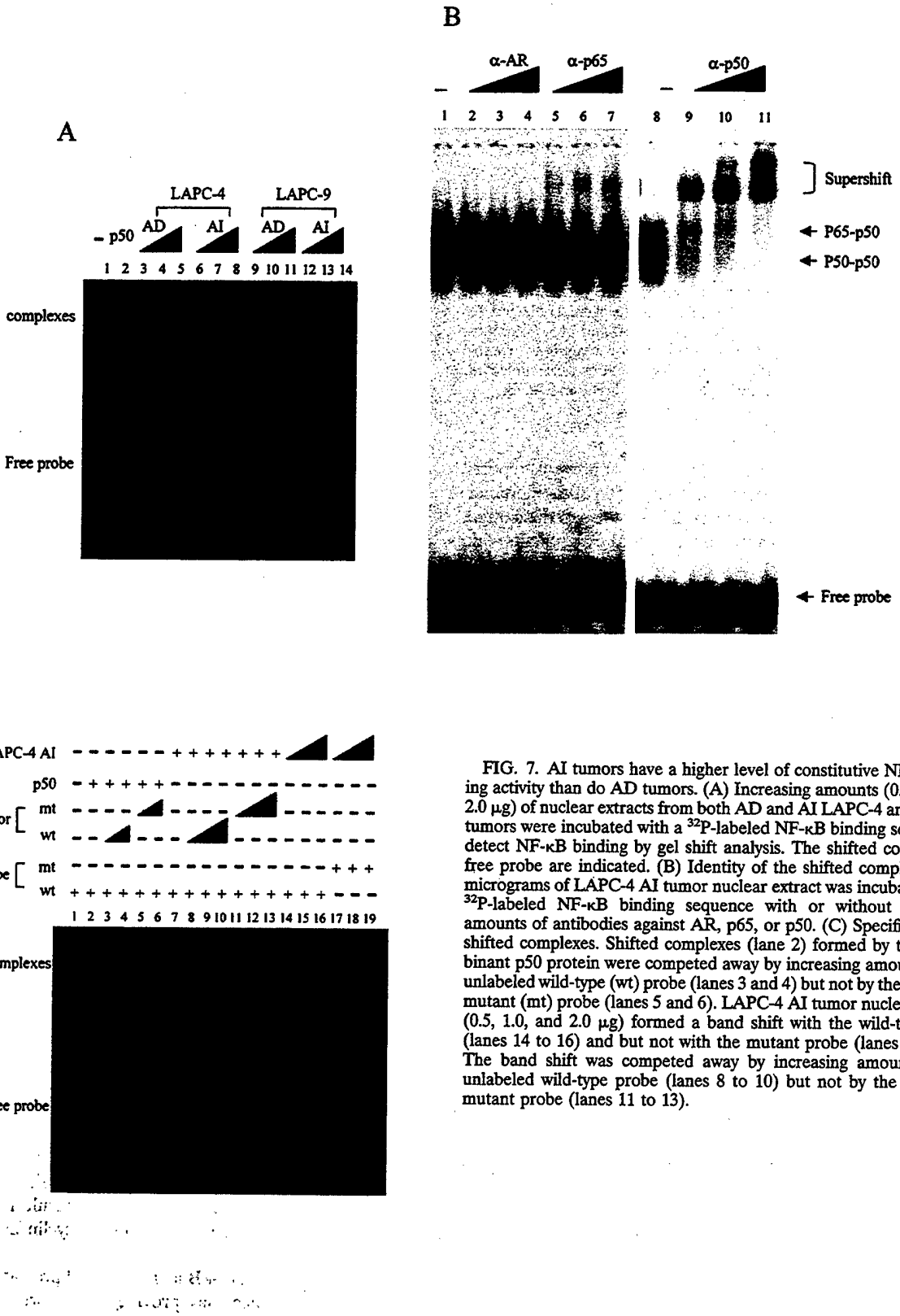

FIG. 7. AI tumors have a higher level of constitutive NF-κB binding activity than do AD tumors. (A) Increasing amounts (0.5, 1.0, and 2.0 μg) of nuclear extracts from both AD and AI LAPC-4 and LAPC-9 tumors were incubated with a ^{32}P-labeled NF-κB binding sequence to detect NF-κB binding by gel shift analysis. The shifted complex and free probe are indicated. (B) Identity of the shifted complexes. Two micrograms of LAPC-4 AI tumor nuclear extract was incubated with a ^{32}P-labeled NF-κB binding sequence with or without increasing amounts of antibodies against AR, p65, or p50. (C) Specificity of the shifted complexes. Shifted complexes (lane 2) formed by the recombinant p50 protein were competed away by increasing amounts of the unlabeled wild-type (wt) probe (lanes 3 and 4) but not by the unlabeled mutant (mt) probe (lanes 5 and 6). LAPC-4 AI tumor nuclear extracts (0.5, 1.0, and 2.0 μg) formed a band shift with the wild-type probe (lanes 14 to 16) and but not with the mutant probe (lanes 17 to 19). The band shift was competed away by increasing amounts of the unlabeled wild-type probe (lanes 8 to 10) but not by the unlabeled mutant probe (lanes 11 to 13).

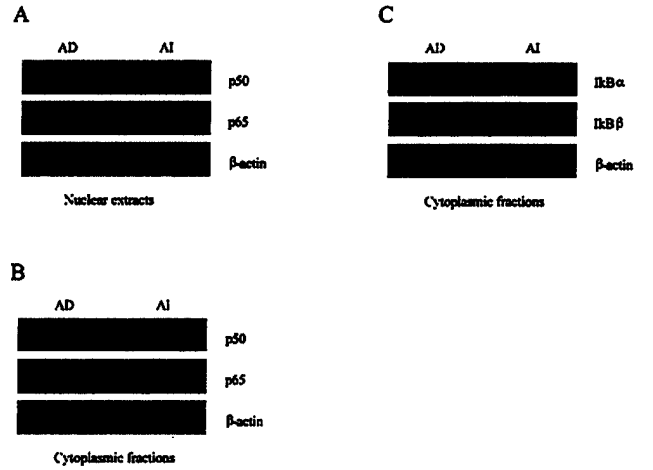

FIG. 8. Western blot analysis of NF-κB and IκB protein levels in LAPC-4 xenograft tumors. (A) Nuclear extracts were subjected to Western blot analysis with antibodies against p50 and p65. (B) Cytoplasmic fractions were subjected to Western blot analysis with antibodies against p50 and p65. (C) Cytoplasmic fractions were subjected to Western blot analysis with antibodies against IκBα and IκBβ.

The band shift pattern was similar to that of previous reports describing the p65/p50 heterodimer and p50/p50 homodimer complexes (10, 29, 41). To confirm the identities of the shifted complexes, we performed antibody supershift experiments with nuclear extracts from LAPC-4 AI tumor tissue. Addition of p65 antibody caused the upper band to shift (Fig. 7B, lanes 5 to 7), and addition of p50 antibody shifted both complexes to higher positions in a dose-dependent fashion (Fig. 7B, lanes 9 to 11). The supershift was specific because antibody against an unrelated protein (AR) did not alter the mobility of the complexes (Fig. 7B, lanes 2 to 4). These results indicated that the upper complex contains the p65/p50 heterodimer and the lower band contains p50.

Binding specificity was determined by using nuclear extracts from LAPC-4 AI tumor tissue. One-half to two micrograms of nuclear extracts produced the band shift with the wild-type probe (Fig. 7C, lanes 14 to 17) but not with a mutant probe (Fig. 7C, lanes 17 to 19). The shifted complex was competed away by a 5- to 80-fold excess of unlabeled wild-type probe (Fig. 7B, lanes 8 to 10) but not by unlabeled mutant probe (Fig. 7C, lanes 11 to 13). The wild-type, but not the mutant, competitor also competed away the shifted complex from recombinant p50 (Fig. 7C, lanes 2 to 6) with comparable efficiency. These results demonstrate an increase in constitutive NF-κB binding activity during progression to androgen independence.

Nuclear accumulation of NF-κB correlates with its binding activity. To examine the mechanism for the elevated NF-κB binding activity in the AI xenografts, we measured the levels of p50, p65, and IκB in nuclear and cytoplasmic extracts of LAPC-4 AD and AI tumors. p50 and p65 protein levels were higher in nuclear extracts and lower in cytoplasmic extracts from AI tumors (Fig. 8A and B). Therefore, the higher NF-κB binding activity in LAPC-4 AI tumor tissue is associated with an increased concentration of NF-κB proteins in the nucleus. We also noted that the level of the IκBβ protein, but not that of the IκBα protein, was lower in cytoplasmic extracts from AI tumor (Fig. 8C), raising the possibility that an increased level of NF-κB in the AI tumor nucleus results from a decreased level of IκBβ in the cytoplasm. A full understanding of the mechanism for increased NF-κB activity in these xenografts requires further study.

DISCUSSION

Our data from analysis of prostate cancer cell lines and xenografts support a role for NF-κB in prostate cancer progression. We demonstrate that NF-κB regulates the expression of PSA, an important clinical marker of prostate cancer progression. We also show that NF-κB directly binds to the PSA core enhancer. By using matched AD and AI prostate cancers derived from two xenograft models, we demonstrated that NF-κB binding activity is upregulated in AI tumors.

Previous work has shown that NF-κB negatively regulates AR function. This conclusion is based on cotransfection studies showing that NF-κB and AR are mutually inhibitory due to competition for a common transcriptional coactivator, CBP (1, 32). Because AR is activated in AI prostate cancer (9, 17, 25), these findings imply an inhibitory role for NF-κB in prostate cancer progression. However, NF-κB inhibition of AR was observed when artificial promoters containing either consensus AR response element (ARE) or NF-κB binding sites were used. Natural promoters are more complex and typically contain *cis*-acting elements for different transcription factors. The PSA core enhancer studied here contains multiple low-affinity AREs that act synergistically (19). Among the four NF-κB binding sites we identified (Fig. 5B), three (I, II, and IV) are adjacent to AREs and NF-κB binding site III overlaps an ARE (19). These observations raise the possibility that cooperative NF-κB and AR binding contributes to PSA transcriptional regulation. Cooperation between nuclear receptors and NF-κB has been demonstrated in other systems (1, 5, 21, 32). For example, retinoid receptors and NF-κB synergistically induce ICAM-1 expression, which promotes metastasis potential (5). NF-κB and the aryl hydrocarbon receptor cooperate to activate c-myc expression in mammary cells (21).

The transition from AD to AI prostate cancer is a multistep process (8). AI cells must first survive androgen deprivation and then grow to become AI tumors. NF-κB may participate in both processes. NF-κB is known to be a critical regulator of survival (3). p65/RelA knockout mice die from extensive liver apoptosis during embryogenesis (4). NF-κB also functions as a survival factor in neurons in response to cell injury through the upregulation of antiapoptotic genes (27). Accumulating evidence indicates that NF-κB also promotes proliferation. Inhibiting NF-κB activation by dominant-negative p65 blocks cell cycle progression in human glioma cells (30). Lymphocytes lacking p50, p65, or c-Rel show defective responses to mitogenic stimulation (12, 24, 39, 40). Inhibiting NF-κB activation by IκBα expression, or by phenylarsine oxide, blocks focus formation in NIH 3T3 cells (15) and colony-forming cell proliferation of acute myelogenous leukemia cells (14). The proliferation-promoting effect of NF-κB may result from its ability to activate c-myc expression (22) and/or cyclin D1 expression (18, 34).

The link between NF-κB activation and prostate cancer androgen independence may provide an opportunity for drug

development. Therapeutic interventions might target upstream pathways that lead to activation of NF-κB, NF-κB itself, or downstream effectors that participate in cancer progression. Because NF-κB is involved in multiple signal transduction pathways, identification of the pathway(s) responsible for increased activity of NF-κB in AI progression will be of great interest.

ACKNOWLEDGMENTS

We thank Genhong Cheng for expression vectors of mutant IκBα, p50, p65, and c-Rel, Michael Carey for wild-type and mutant PSA-P/E–Luc reporters, and Katherine Ellwood for assistant in DNase I footprinting and EMSA. We also thank Ke Shuai, Mitch Gross, and Ingo Mellinghoff for critical reading of the manuscript.

This work was supported by a postdoctoral award from the DOD (C.D.C.) and by grants from the DOD, the NCI, and CaPCure (C.L.S.)

REFERENCES

1. **Aarnisalo, P., H. Santti, H. Poukka, J. J. Palvimo, and O. A. Janne.** 1999. Transcription activating and repressing functions of the androgen receptor are differentially influenced by mutations in the deoxyribonucleic acid binding domain. Endocrinology **140**:3097–3105.
2. **Abreu-Martin, M. T., A. Chari, A. A. Palladino, N. A. Craft, and C. L. Sawyers.** 1999. Mitogen-activated protein kinase kinase kinase 1 activates androgen receptor-dependent transcription and apoptosis in prostate cancer. Mol. Cell. Biol. **19**:5143–5154.
3. **Baldwin, A. S., Jr.** 2001. Series introduction: the transcription factor NF-κB and human disease. J. Clin. Investig. **107**:3–6.
4. **Beg, A. A., W. C. Sha, R. T. Bronson, S. Ghosh, and D. Baltimore.** 1995. Embryonic lethality and liver degeneration in mice lacking the RelA component of NF-κB. Nature **376**:167–170.
5. **Chadwick, C. C., L. J. Shaw, and R. C. Winneker.** 1998. TNF-α and 9-*cis*-retinoic acid synergistically induce ICAM-1 expression: evidence for interaction of retinoid receptors with NF-κB. Exp. Cell Res. **239**:423–429.
6. **Chen, C. D., and D. M. Helfman.** 1999. Donor site competition is involved in the regulation of alternative splicing of the rat β-tropomyosin pre-mRNA. RNA **5**:290–301.
7. **Cleutjens, K. B., H. A. van der Korput, C. C. Ehren-van Eekelen, R. A. Sikes, C. Fasciana, L. W. Chung, and J. Trapman.** 1997. A 6-kb promoter fragment mimics in transgenic mice the prostate-specific and androgen-regulated expression of the endogenous prostate-specific antigen gene in humans. Mol. Endocrinol. **11**:1256–1265.
8. **Craft, N., C. Chhor, C. Tran, A. Belldegrun, J. DeKernion, O. N. Witte, J. Said, R. E. Reiter, and C. L. Sawyers.** 1999. Evidence for clonal outgrowth of androgen-independent prostate cancer cells from androgen-dependent tumors through a two-step process. Cancer Res. **59**:5030–5036.
9. **Craft, N., Y. Shostak, M. Carey, and C. L. Sawyers.** 1999. A mechanism for hormone-independent prostate cancer through modulation of androgen receptor signaling by the HER-2/neu tyrosine kinase. Nat. Med. **5**:280–285.
10. **Davis, J. N., O. Kucuk, and F. H. Sarkar.** 1999. Genistein inhibits NF-κB activation in prostate cancer cells. Nutr. Cancer **35**:167–174.
11. **Dickens, M., J. S. Rogers, J. Cavanagh, A. Raitano, Z. Xia, J. R. Halpern, M. E. Greenberg, C. L. Sawyers, and R. J. Davis.** 1997. A cytoplasmic inhibitor of the JNK signal transduction pathway. Science **277**:693–696.
12. **Doi, T. S., T. Takahashi, O. Taguchi, T. Azuma, and Y. Obata.** 1997. NF-κB RelA-deficient lymphocytes: normal development of T cells and B cells, impaired production of IgA and IgG1 and reduced proliferative responses. J. Exp. Med. **185**:953–961.
13. **Ellwood, K., W. Huang, R. Johnson, and M. Carey.** 1999. Multiple layers of cooperativity regulate enhanceosome-responsive RNA polymerase II transcription complex assembly. Mol. Cell. Biol. **19**:2613–2623.
14. **Estrov, Z., S. K. Manna, D. Harris, Q. Van, E. H. Estey, H. M. Kantarjian, M. Talpaz, and B. B. Aggarwal.** 1999. Phenylarsine oxide blocks interleukin-1β-induced activation of the nuclear transcription factor NF-κB, inhibits proliferation, and induces apoptosis of acute myelogenous leukemia cells. Blood **94**:2844–2853.
15. **Finco, T. S., J. K. Westwick, J. L. Norris, A. A. Beg, C. J. Der, and A. S. Baldwin, Jr.** 1997. Oncogenic Ha-Ras-induced signaling activates NF-κB transcriptional activity, which is required for cellular transformation. J. Biol. Chem. **272**:24113–24116.
16. **Ghosh, S., M. J. May, and E. B. Kopp.** 1998. NF-κB and Rel proteins: evolutionarily conserved mediators of immune responses. Annu. Rev. Immunol. **16**:225–260.
17. **Gregory, C. W., R. T. Johnson, Jr., J. L. Mohler, F. S. French, and E. M. Wilson.** 2001. Androgen receptor stabilization in recurrent prostate cancer is associated with hypersensitivity to low androgen. Cancer Res. **61**:2892–2898.
18. **Guttridge, D. C., C. Albanese, J. Y. Reuther, R. G. Pestell, and A. S. Baldwin, Jr.** 1999. NF-κB controls cell growth and differentiation through transcriptional regulation of cyclin D1. Mol. Cell. Biol. **19**:5785–5799.
19. **Huang, W., Y. Shostak, P. Tarr, C. Sawyers, and M. Carey.** 1999. Cooperative assembly of androgen receptor into a nucleoprotein complex that regulates the prostate-specific antigen enhancer. J. Biol. Chem. **274**:25756–25768.
20. **Keller, E. T., C. Chang, and W. B. Ershler.** 1996. Inhibition of NF-κB activity through maintenance of IκBα levels contributes to dihydrotestosterone-mediated repression of the interleukin-6 promoter. J. Biol. Chem. **271**: 26267–26275.
21. **Kim, D. W., L. Gazourian, S. A. Quadri, R. Romieu-Mourez, D. H. Sherr, and G. E. Sonenshein.** 2000. The RelA NF-κB subunit and the aryl hydrocarbon receptor (AhR) cooperate to transactivate the c-myc promoter in mammary cells. Oncogene **19**:5498–5506.
22. **Kim, D. W., M. A. Sovak, G. Zanieski, G. Nonet, R. Romieu-Mourez, A. W. Lau, L. J. Hafer, P. Yaswen, M. Stampfer, A. E. Rogers, J. Russo, and G. E. Sonenshein.** 2000. Activation of NF-κB/Rel occurs early during neoplastic transformation of mammary cells. Carcinogenesis **21**:871–879.
23. **Klein, K. A., R. E. Reiter, J. Redula, H. Moradi, X. L. Zhu, A. R. Brothman, D. J. Lamb, M. Marcelli, A. Belldegrun, O. N. Witte, and C. L. Sawyers.** 1997. Progression of metastatic human prostate cancer to androgen independence in immunodeficient SCID mice. Nat. Med. **3**:402–408.
24. **Kontgen, F., R. J. Grumont, A. Strasser, D. Metcalf, R. Li, D. Tarlinton, and S. Gerondakis.** 1995. Mice lacking the c-rel proto-oncogene exhibit defects in lymphocyte proliferation, humoral immunity, and interleukin-2 expression. Genes Dev. **9**:1965–1977.
25. **Linja, M. J., K. J. Savinainen, O. R. Saramaki, T. L. Tammela, R. L. Vessella, and T. Visakorpi.** 2001. Amplification and overexpression of androgen receptor gene in hormone-refractory prostate cancer. Cancer Res. **61**:3550–3555.
26. **Miyamoto, S., and I. M. Verma.** 1995. Rel/NF-κB/I κB story. Adv. Cancer Res. **66**:255–292.
27. **Moerman, A. M., X. Mao, M. M. Lucas, and S. W. Barger.** 1999. Characterization of a neuronal κB binding factor distinct from NF-κB. Brain Res. Mol. Brain Res. **67**:303–315.
28. **Muenchen, H. J., D. L. Lin, M. A. Walsh, E. T. Keller, and K. J. Pienta.** 2000. Tumor necrosis factor-α-induced apoptosis in prostate cancer cells through inhibition of nuclear factor-κB by an IκBα "super-repressor." Clin. Cancer Res. **6**:1969–1977.
29. **Nakshatri, H., P. Bhat-Nakshatri, D. A. Martin, R. J. Goulet, Jr., and G. W. Sledge, Jr.** 1997. Constitutive activation of NF-κB during progression of breast cancer to hormone-independent growth. Mol. Cell. Biol. **17**:3629–3639.
30. **Otsuka, G., T. Nagaya, K. Saito, M. Mizuno, J. Yoshida, and H. Seo.** 1999. Inhibition of nuclear factor-κB activation confers sensitivity to tumor necrosis factor-α by impairment of cell cycle progression in human glioma cells. Cancer Res. **59**:4446–4452.
31. **Palayoor, S. T., M. Y. Youmell, S. K. Calderwood, C. N. Coleman, and B. D. Price.** 1999. Constitutive activation of IκB kinase α and NF-κB in prostate cancer cells is inhibited by ibuprofen. Oncogene **18**:7389–7394.
32. **Palvimo, J. J., P. Reinikainen, T. Ikonen, P. J. Kallio, A. Moilanen, and O. A. Janne.** 1996. Mutual transcriptional interference between RelA and androgen receptor. J. Biol. Chem. **271**:24151–24156.
33. **Pang, S., J. Dannull, R. Kaboo, Y. Xie, C. L. Tso, K. Michel, J. B. deKernion, and A. S. Belldegrun.** 1997. Identification of a positive regulatory element responsible for tissue-specific expression of prostate-specific antigen. Cancer Res. **57**:495–499.
34. **Rayet, B., and C. Gelinas.** 1999. Aberrant rel/nfkb genes and activity in human cancer. Oncogene **18**:6938–6947.
35. **Sambrook, J., E. Fritsch, and T. Maniatis.** 1989. Molecular cloning: a laboratory manual, 2nd ed. Cold Spring Harbor Laboratory Press, Cold Spring Harbor, N.Y.
36. **Schuur, E. R., G. A. Henderson, L. A. Kmetec, J. D. Miller, H. G. Lamparski, and D. R. Henderson.** 1996. Prostate-specific antigen expression is regulated by an upstream enhancer. J. Biol. Chem. **271**:7043–7051.
37. **Sen, R., and D. Baltimore.** 1986. Inducibility of κ immunoglobulin enhancer binding protein NF-κB by a posttranslational mechanism. Cell **47**:921–928.
38. **Sen, R., and D. Baltimore.** 1986. Multiple nuclear factors interact with the immunoglobulin enhancer sequences. Cell **46**:705–716.
39. **Sha, W. C., H. C. Liou, E. I. Tuomanen, and D. Baltimore.** 1995. Targeted disruption of the p50 subunit of NF-κB leads to multifocal defects in immune responses. Cell **80**:321–330.
40. **Snapper, C. M., P. Zelazowski, F. R. Rosas, M. R. Kehry, M. Tian, D. Baltimore, and W. C. Sha.** 1996. B cells from p50/NF-κB knockout mice have selective defects in proliferation, differentiation, germ-line CH transcription, and Ig class switching. J. Immunol **156**:183–191.
41. **Van Antwerp, D. J., S. J. Martin, T. Kafri, D. R. Green, and I. M. Verma.** 1996. Suppression of TNF-α-induced apoptosis by NF-κB. Science **274**:787–789.
42. **Zabel, U., R. Schreck, and P. A. Baeuerle.** 1991. DNA binding of purified transcription factor NF-κB. Affinity, specificity, Zn^{2+} dependence, and differential half-site recognition. J. Biol. Chem. **266**:252–260.